



**POLITECNICO
DI TORINO**

HYPERSPECTRAL IMAGING OF BLACK MICROPLASTIC IN WATER

Master Thesis Report

Presented by

Hafiz Ramzan Mubarak

and defended at

Politecnico di Torino, Italy

Host Supervisor:

Prof. Matthieu Roussey

Host University

University of Eastern Finland

Academic Supervisor:

PhD, Carlo Ricciardi

Torino, 2023

Abstract

Environmental pollution by microplastics is now recognized as an issue with strong possible impact on ecology, society, and economy. Black microplastics (BMPs) have attracted attention due to their prolonged existence and potential for toxicity. This thesis investigates the utilization of hyperspectral imaging (HSI) techniques for detecting and characterizing black microplastics (BMPs) in water samples directly.

The thesis begins by introducing the issue of microplastic pollution, emphasizing the importance of distinguishing BMPs from natural particles. Hyperspectral imaging, known for its ability to capture both spatial and spectral information, is proposed as a promising approach to address this challenge.

A comprehensive overview of hyperspectral imaging techniques, including point scanning, line scanning, and focal plane array (FPA) scanning, is presented. The principles of hyperspectral cameras, such as optics, detectors, and spectral dispersing elements, are discussed. Additionally, specific data acquisition and processing techniques applicable to hyperspectral imaging are examined.

The experimental procedures section describes the materials and methods used in the study, including the use of various BMP concentrations in water. The thesis describes the measurements and calculations used to analyze the hyperspectral data, with a focus on BMP reflectance and transmittance.

The results and discussion section presents the findings from the experiments and provides a comprehensive analysis of BMPs in water. The thesis explores the reflectance and transmittance characteristics of BMPs, contributing to their characterization in aquatic environments.

In conclusion, this thesis showcases how hyperspectral imaging serves as an effective means to identify and characterize black microplastics in water. By capturing intricate spectral details, HSI facilitates the recognition and analysis of BMPs within intricate environmental samples. The outcomes of this study hold the potential to provide guidance for future initiatives aimed at monitoring microplastic pollution, thereby playing a vital role in safeguarding ecosystems.

Acknowledgement

I am deeply thankful to the PSRS Consortium for granting me the EMJMD scholarship, which has transformed my aspiration of participating in an Erasmus Mundus Joint master's degree program into a concrete reality. Their support has been invaluable in facilitating this remarkable opportunity.

I would like to express my sincere appreciation to my supervisor at the University of Eastern Finland for their exceptional guidance throughout this project. Their support and expertise have been crucial in the successful completion of this work.

Furthermore, I am grateful to the professors and instructors at Université Jean Monnet, the University of Eastern Finland, and Politecnico di Torino for their continuous guidance and assistance during my academic journey. Their knowledge and mentorship have greatly contributed to my growth and development.

To my seniors, friends, and family, I want to extend my heartfelt gratitude for your unwavering support throughout this journey. Your presence and encouragement have been a constant source of motivation, and I am deeply appreciative of your impact on my life.

Table of Content

1	Introduction	1
2	Black Micro Plastic (BMP).....	5
3	Hyperspectral imaging (HSI).....	9
3.1	Point scanning.....	11
3.2	Line Scanning	12
3.3	Focal plane array (FPA) and Scanning.....	15
3.4	Hyperspectral camera.....	16
3.4.1	Working principle.	16
3.4.2	Optics	16
3.4.3	Detector	16
3.4.4	Spectral dispersing element	17
3.4.5	Data acquisition:.....	18
3.4.6	Data Processing.....	19
3.5	Fourier transform infrared (FTIR) Imaging	20
3.5.1	Transmission imaging	20
3.5.2	Attenuated total reflection imaging.....	21
3.6	FPA-FTIR vs hyperspectral camera.....	21
4	Material and Methods.....	23
4.1	Sample preparation	23
4.2	Methods.....	25
4.2.1	Point scan measurement	25
4.2.2	Hyperspectral imaging.....	27
5	Results and discussion	29
5.1	Point scanning.....	29
5.1.1	Black macro plastics in air	29
5.1.2	Black micro plastics in water	31
5.2	Hyperspectral Imaging.....	40
5.2.1	Hyperspectral imaging of black macro plastic in air	41
5.2.2	Hyperspectral imaging of black microplastic in water	43

6 **Conclusion**.....55

7 **Bibliography**56

1 Introduction

Plastics are synthetic polymer compound which may contain other chemical to enhance performance. They have usually a relatively high molecular mass, and are, moreover, insoluble in water used in many industries. It has been reported that the production has been reach up to 280 million tones yearly [1], [2]. Excess demand and production of plastics turned into serious health and environmental problems [3]. If some plastics are biodegradable, many of them remain for long time until breaking into smaller pieces becoming the micro- or nanoplastics [4].

Microplastics (MPs) are defined as plastic fragments which are smaller than 5 mm in any dimensions. Nanoplastics are items <100nm in any dimensions [5]. Microplastics can be categorized into two distinct groups: primary and secondary. Primary MPs are manufactured items at micro size including microsphere (< 500 μm) contained in cosmetics products etc. Secondary MPs are coming from the degradation of larger plastics pieces which turn into micro or nano plastics[5]. They can also be classified based on their physical structure, which includes fibers and fragments, as well as their chemical composition. For instance, examples of different types include Nylon, polyethylene (PE), low-density PE (LDPE), PE terephthalate (PET), polyacrylates (PA), polypropylene (PP), Polystyrene (PS), acrylic (AC), PVC, and polyester (PES) [6].

Microplastics (MPs) can have both direct and indirect effects on aquatic organisms. These organisms might ingest larger plastic particles, potentially resulting in suffocation, reduced ability to acquire proper nutrition, false satiation, starvation, and ultimately the demise of certain species [7]. The significant concern lies in the fact that these plastics are not easily removable from habitats and can be consumed by aquatic species. This becomes problematic as these species are also part of the human food chain, which can consequently lead to health issues. In short, Humans are exposed to both plastic particles and chemical additives consuming sea foods[8].

There are several techniques for detecting microplastics in the environment. Initially, plastic particles or particles suspected to be plastic are extracted from the

environmental samples. These extracted particles are then subjected to both physical and chemical analysis to confirm the presence of plastics [9].

Historically, microplastics have been separated from sand or sediments with higher densities through a process called density separation. Once separated, the physical shape of microplastics can be examined using microscopy, while the identification of specific compounds is commonly achieved by Raman and Fourier transform infrared spectroscopies (FT-IR) [10][11].

Hyperspectral imaging is employed, encompassing many spatial pixels and a multitude of spectral bands that range from visible to infrared wavelengths. This method facilitates the assessment of the chemical composition of individual spatial pixels by analyzing their unique spectral data. Hyperspectral imaging technology has been employed to detect plastic pollution in filtrates of seawater. To prepare for hyperspectral imaging, the microplastics present in the soil samples were isolated and identified using Raman spectroscopy. Hyperspectral images were captured of soil samples containing microplastics, along with samples of boulders, wilted leaves, fresh leaves, and branches[12].

Black polymers, commonly employed for specialized applications with specific requirements, encompass a wider range of materials compared to regular household plastic waste. Approximately 0.5 to 3 percent of the mass of black polymers consists of soot or black masterbatch[13]. The presence of various additives, such as fibers, or soot, can significantly alter the spectra of these polymers, thereby complicating their identification. These additives and fillers are incorporated into plastics to achieve specific properties. To tackle the characterization of black polymers, various infrared (IR) techniques have been developed. These encompass attenuated total reflection (ATR) [14], [15], infrared transmission [16], emission spectroscopy [17], and photoacoustic spectroscopy [18]. These techniques have been specifically designed to fulfill the need for precise characterization of black polymers [13].

Our main focus is on black microplastics using hyperspectral imaging technique to identify the black microplastics directly in water, i.e., without prior

filtering or sorting. The black microplastics are less detectable as compared to other colored plastic due to more absorption of light.

For non-black polymers, near infrared spectroscopy (NIRS) provides a quick and accurate identification[19]. Polymers and different waste products can be discriminate base on wavelength ranges[20], therefore, near infrared spectroscopy (NIRS) is very useful technique to identify different type of polymers such PP, PS, and PE at different wavelength ranges [21] but to study black microplastic, it requires a wavelength range.

Identifying black microplastics (BMPs) presents a challenge when employing specific techniques. This challenge arises primarily from their substantial light absorption, which mandates the use of broader wavelength ranges for accurate detection. As a result, the quantity and proportion of black microplastics within the general plastic presence in the environment often face underestimation compared to other colored plastics [22]. Among the 50 surveyed articles, a significant majority centered their attention on polypropylene and polyethylene as the prevailing polymers found in microplastics [22]. Interestingly, not a single article furnished details regarding the molecular structure of MPs with respect to colors. The absence of consistent methodologies among microplastic researchers and the complexities linked with classifying and identifying black microplastics have resulted in significant challenges. Fundamental queries, including the prevalent types of black microplastics, their abundance, and potential sources, remain unanswered. These knowledge gaps underscore the urgency for enhanced techniques and standardization in microplastic research [22].

Raman spectroscopy offers a more precise method for the detection of microplastic particles, even those smaller than one micrometer in size. This technique involves coupling a Raman spectrometer with a microscope, enabling the analysis of tiny particles. Offering an extensive spectral range, it is especially well-suited for plastic identification. Through the comparison of Raman peak positions and shapes with an established microplastics database, precise identification can be accomplished. Raman spectroscopy can detect particles as small as 10 micrometers in size and wave range between $10\text{-}4000\text{ cm}^{-1}$ which is useful for black MPs[23].

FT-IR (Fourier Transform Infrared) spectroscopy is another valuable technique for identifying microplastics. It relies on the absorption peaks of plastic in the infrared range. FT-IR spectroscopy enables effective microplastic identification and facilitates the comparison of sample spectra with a recognized microplastics database. However, it does not offer quantitative microplastic identification, and the presence of overlapping peaks and troughs in the spectra can obscure specific characteristics [6].

Transmission spectroscopy is a method based on the simple transmission of spectra from samples. It does not provide quantitative identification of microplastics but can be useful for initial screening purposes[24].

Hyperspectral imaging is a technique used for both imaging the shape of microplastic particles and determining their spectra simultaneously. This method allows for a comprehensive analysis of microplastics[25].

This thesis presents a comprehensive exploration of point scanning and hyperspectral imaging techniques, aiming to efficiently identify black microplastics within air and water samples. Our research delves deeply into the intricacies of transmittance and reflectance spectra, unraveling hidden patterns in the context of black microplastics. Notably, our study extends its reach to include a quantitative assessment of different BMP concentrations within water samples, shedding light on their prevalence. The significance of our findings transcends the academic realm. By enhancing the black microplastic identification, this research contributes valuable insights to ongoing discussions about environmental sustainability and human well-being. As concerns surrounding microplastic pollution intensify, the knowledge gained from our study aids in formulating effective strategies and informed decision-making. Through meticulous exploration of point scanning and hyperspectral imaging methods, detailed spectral analysis, and quantitative evaluation of black microplastic concentrations, our work contributes to the global effort of mitigating microplastic pollution's impact on both ecosystems and human life.

2 Black Micro Plastic (BMP)

Plastics hold a prominent position across numerous industries owing to their cost-effectiveness in production, remarkable durability, inherent flexibility, non-reactive attributes, and excellent insulating capabilities. Their versatile applications span a wide array of sectors, encompassing healthcare, packaging, electronics, construction, agriculture, communication, and transportation [26].

From optical properties point of view, plastic materials commonly exhibit refractive indices that fall within the range of 1.45 to 1.70 in the visible, although this range can be extended to 1.2 to 1.9. In conditions without light scattering, these materials are capable of transmitting around 80-90 percent of the incoming light. This transmission behavior stems from the distinct refractive index differential between the spherulites and the amorphous regions. Consequently, amorphous polymers are recognized for their efficient light transmission. On the other hand, crystalline polymers often possess characteristics of being either white and opaque or translucent [27].

Plastics can be imbued with color using a range of methods such as pigments, dyes, and substrates. Pigments, existing in powdered form and insoluble in their medium, offer dual benefits of tinting and covering power. Dyes, comprising intricate organic compounds that dissolve in polymers, disperse molecularly within the material, retaining transparency. Additives, when functioning as dyes, selectively absorb undesirable wavelengths. Substrates, on the other hand, involve organic pigments or dyes that are adhered to a supportive material. These color-enhancing mechanisms are categorized based on their origin and properties. They demand a particle size surpassing the wavelength of light and a notably high refractive index. These characteristics collectively determine the interaction of the colored plastics with light, allowing them to display an array of vivid and visually appealing hues [27].

A variety of organic pigments, encompassing carbon blacks, phthalocyanines, quinacridones, and azo pigments, find widespread application in plastics, effectively augmenting physical attributes and offering an extensive spectrum of colors. Carbon blacks, notably, are among the most frequently employed pigments. Renowned for their potent pigmentation properties, carbon blacks significantly enhance multiple

physical qualities of polymers. These enhancements span light stability, processability, and mechanical attributes. Quinacridones are gaining popularity as organic pigments in the realm of plastics. Their increasing use is attributed to their commendable stability against both light and heat, their resistance to migration, and their resilience against various chemicals [27]. Carbon black, extending beyond its conventional applications, is also harnessed for its ability to address antistatic properties. It further plays a pivotal role in the creation of cable covers, wires, and materials utilized for electromagnetic interference shielding (EMI) [28]. The multi-faceted applications of these organic pigments illustrate their pivotal role in enhancing both the aesthetics and functionality of plastic materials.

Although the chemistry of black plastic is not essentially distinct from that of other colored plastics, black plastic can contain extra additives. Carbon black, for example, is a common pigment used to make black plastic. Carbon black is generated by burning hydrocarbons in the absence of air and is used to improve the plastic's properties, such as its resistance to UV radiation and heat, as well as provide black color. The pigments are typically classified based on their manufacturing method as furnace, lamp, thermal, or acetylene blacks[29].

The wavelength of light absorbed or reflected by plastic is mainly determined by the type of pigment or dye used to color the plastic. However, black plastic tends to absorb more light across the visible spectrum compared to other colors, as it typically contains high levels of carbon black pigment. It is highly effective in absorbing light across a wide range of wavelengths, from UV to IR radiation. This implies that black plastic will absorb a greater amount of light across the entire visible spectrum in contrast to other colored plastic. On the other hand, other colors of plastic may reflect or transmit more light in certain parts of the visible spectrum, depending on the specific pigments or dyes used to color the plastic. For instance, blue plastic may reflect more blue light, while red plastic may reflect more red light.

Extensive research has revealed that polyethylene (PE) and polypropylene (PP) can be effectively differentiated by their distinctive response to mid-infrared and long-infrared. When subjected to mid-wave infrared (MWIR) radiation, PE generates two distinctive spectral features, whereas PP produces four. Notably, PP exhibits a

unique absorption band at 2725 cm^{-1} , setting it apart, while PE is characterized by a distinctive 70 cm^{-1} wide gap.

In the LWIR range, PP showcases multiple medium peaks distributed between 800 and 1170 cm^{-1} . In contrast, polyethylene elicits a singular, specific peaks that resides near the lower boundary of LWIR. However, it is important to acknowledge that the accuracy of identification can be influenced by the sensitivity of the equipment utilized [30]. This research not only sheds light on the differentiation between these polymers but also emphasizes the significance of precise equipment calibration for ensuring accurate identification outcomes.

In summary, polyethylene (PE) stands out due to the absence of spectral features in both MWIR and LWIR. On the other hand, polypropylene exhibits more signals, primarily falling within the same ranges. This commonality arises from the fact that both materials primarily consist of C-C and C-H bonds, disregarding impurities, aging, and additives [30].

Likewise, when considering other polymers like Ethylene Vinyl Acetate (EVA) and Cross-linked (X) Polyethylene (PEX), their MWIR profiles bear resemblance to polyethylene (PE). However, the LWIR region offers the capability to distinguish EVA from PE, although the same distinction is not applicable to PEX.

In contrast, Polyvinyl chloride (PVC) and Polyoxymethylene exhibit MWIR spectra akin to PE, albeit with distinctively curved shapes at slightly varied wavenumbers. It is in their long IR spectra that these two polymers become easily discernible, allowing for straightforward identification [30]. This comprehensive differentiation emphasizes the role of infrared spectra in polymer characterization, providing a powerful tool for accurate material identification.

Black carbon, or carbon black, absorbs more light due to its highly porous and functionalized molecular structure. The surface of carbon black particles is covered with various functional groups, including hydroxyl, carboxyl, and carbonyl, which interact with light energy, resulting in the absorption of photons across a broad range of wavelengths. The highly porous structure of carbon black particles also allows them to trap and absorb light energy, rather than allowing it to pass through the material, making them more effective in absorbing light than other colors of plastic.

Consequently, black plastics absorb a more significant amount of light across the whole visible spectrum compared to other colors of plastic due to carbon black's unique properties. Carbon black exhibits a robust absorption of wavelengths spanning from ultraviolet to near-infrared. Presently, techniques like near-infrared hyperspectral imagery struggle to differentiate black microplastics [31].

Both carbon dioxide and water, atmospheric constituents, exhibit detectable presence within both mid Infrared and long Infrared spectral domains. The MWIR range spans roughly 5000 to 2000 cm^{-1} or 2 to 5 μm , while the LWIR range encompasses around 1350 to 700 cm^{-1} or 7.4 to 14.0 μm . Importantly, the existence of these atmospheric species is not anticipated to interfere with polymer identification, as the covered spectral ranges and signal characteristics distinctly differ [32]. This knowledge underscores the feasibility of effectively distinguishing between atmospheric constituents and polymer materials using infrared spectroscopy techniques.

3 Hyperspectral imaging (HSI)

Hyperspectral imaging has garnered significant attention from numerous research groups for its potential in detecting both macro and microplastics. One notable study, conducted by Blasi M [33], employed short-wave infrared (SWIR) spectral imaging spanning the range of 900 nm to 1700 nm. The research primarily centered on characterizing diverse polymer types, encompassing polyethylene variants HDPE, LDPE as well as PP, PVC, PS, for macro plastic identification. In a similar vein, the work of author Hibbitts [34] harnessed hyperspectral imaging to pinpoint two specific infrared bands capable of effectively discriminating plastic objects, such as fiberglass and polyesters. They capitalized on the first harmonic of the vibrational carbon and hydrogen absorption band within the wavelength range of 1650-1750 nm. Another research endeavor by Moroni [35] employed hyperspectral imaging to recycle and separate PET and PVC across various stages of their life cycle. Their exploration encompassed both the visible range (400-1000 nm) and SWIR range (900-1700 nm). Intriguingly, the visible-range wavebands proved less effective in distinguishing between PET and PVC due to their color-dependent nature. Instead, the researchers employed the ratio of absorbance values at 1656 nm and 1712 nm as a discriminating factor. Chuczko [36] conducted an in-depth exploration into the utilization of neural networks for the detection of microplastics within hyperspectral images obtained from natural environments. In parallel, Serranti [37] engaged in a discussion about the effective deployment of hyperspectral imaging in the wavelength range of 1000 to 2500 nm. This approach was complemented by the integration of chemometric techniques, aiding in the identification of polymers within samples acquired from a wide array of marine environments. These two studies showcase the innovative fusion of advanced technologies and analytical methods, further advancing our capabilities in understanding and addressing plastic pollution challenges. A comprehensive investigation led by the SOC710-SWIR hyperspectral imaging system [38] explored thirteen distinct plastic samples commonly encountered in everyday use and general plastic waste. The study's focal point was to exhibit the distinguishability of these samples through the application of hyperspectral image data and spectral indices as features. Collectively, these studies

underscore the growing prominence of hyperspectral imaging as a pivotal tool in unraveling the complex world of plastic identification and characterization. Raman spectroscopy provides precise and accurate results over a significant spectral range of 50 cm^{-1} , making it one of the most precise methods for analyzing microplastics. However, it is important to note that this spectroscopic technique generates a weak Raman signal, and its sample preparation process requires laborious efforts. As a result, it is recommended that only experts with knowledge in Raman spectroscopy utilize this technique[6].

HSI has emerged as a contemporary technique for the detection and identification of microplastic particles (MNP). This approach enables the concurrent analysis of a particle's morphology and its identification through its distinctive spectral traits. However, the acquisition of meaningful insights necessitates comprehensive data processing, owing to the substantial data files generated by hyperspectral cameras. Often, this processing leverages machine learning methodologies, incorporating techniques such as principal component analysis or other forms of classification [24]. The holistic process of HSI is encapsulated in Figure 1 [39], highlighting the systematic steps involved in this advanced scheme.

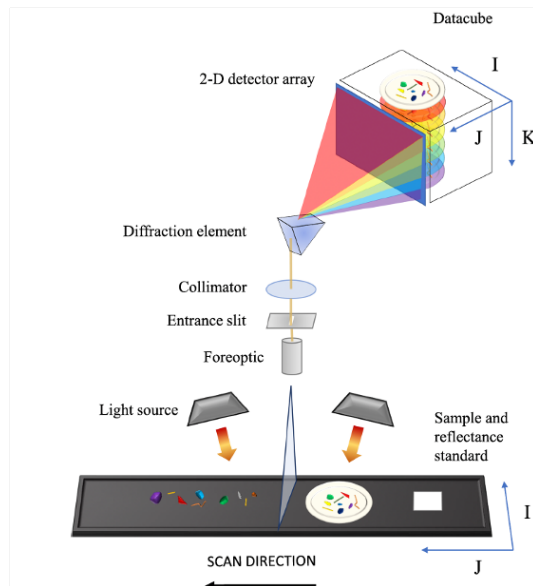


Figure 1: A diagram illustrating the application of HSI for the purpose of examining MP. Figure reprinted from [39].

The creation of multivariate and hyperspectral images relies on a range of physics principles. One notable illustration of these principles in action is the generation of Near-Infrared (NIR) optical images [40]. A conventional spectrophotometer typically comprises essential components: a light source, a monochromator or filter system for dispersing light into distinct wavelength bands, a sample presentation unit, and a detection system encompassing a detector alongside digitization and storage hardware and software.

For generating broad-spectrum NIR radiation, tungsten halogen or xenon gas plasma lamps are widely used sources. Alternatively, light-emitting diodes and tunable lasers can be employed for illumination, offering narrower wavelength bands. However, achieving coverage across the complete NIR spectral range (780-2500 nm) requires the use of multiple diodes or lasers [41]. The dispersion of spectrum energy can be effectively achieved through the utilization of a grating device. In addition, scanning interferometers offer a valuable approach for capturing NIR spectra from a single point.

In the realm of hyperspectral imaging, a dedicated spectrometer camera combines hardware designed for capturing spectral data with supplementary components for gathering spatial information. Spatial data acquisition is facilitated through various means, including the utilization of spectrometer optics, controlled sample positioning, or a synergistic combination of both strategies. The selection of camera configurations hinges on the nature of spatial information sought, resulting in three fundamental options: point scan, line scan, or plane scan [42]. This harmonious fusion of hardware and methodologies establishes a foundation for capturing intricate details encompassing both spectral and spatial dimensions within the realm of hyperspectral imaging.

3.1 Point scanning

The process of scanning black plastic with a spectrometer or similar device involves analyzing the reflected or transmitted light from black plastic material at specific points. This technique collects spectral data, which provides valuable insights into the optical properties and characteristics of black plastic.

To perform point scanning of black plastic, several key points should be considered. Firstly, the selection of an appropriate spectrometer is crucial, ensuring it can measure the desired spectral range with the required resolution and sensitivity for accurate data collection. In this thesis spectral range is used from 250nm to 2500nm.

Sample preparation is essential to obtain reliable results. The black plastic sample should be free from contamination and reflections that could interfere with measurements. To ensure consistency, the sample should ideally be flat and uniform.

The spectrometer probe or sensor is positioned at specific points on the black plastic surface during the point scanning process. Depending on the measurement setup, the probe is either in direct contact or at a fixed distance. Spectral data is recorded from each scanned point by measuring the reflected or transmitted light.

The spectral data collected consists of intensity or reflectance values at various wavelengths or frequency bands. This data is then analyzed to identify patterns, variations, or specific characteristics related to the black plastic material. Comparing spectral signatures, calculating reflectance or absorption coefficients, or extracting specific parameters of interest are all examples of analysis techniques.

The interpretation of the spectral information unveils insights into the optical properties and distinctive attributes of black plastics. This invaluable data serves a multitude of purposes, encompassing quality control, precise material identification, comprehensive surface characterization, and the ability to track changes occurring over time.

3.2 Line Scanning

Line-scan hyperspectral imaging can be tailored in diverse configurations to address precise detection needs. Within line-scan hyperspectral imaging techniques, two core modes are commonly employed: reflection and transmission measurements. These modes will be elaborated upon in subsequent sections of this thesis. For a visual depiction of the line scan camera setup and an internal camera view, please refer to Figure 2.

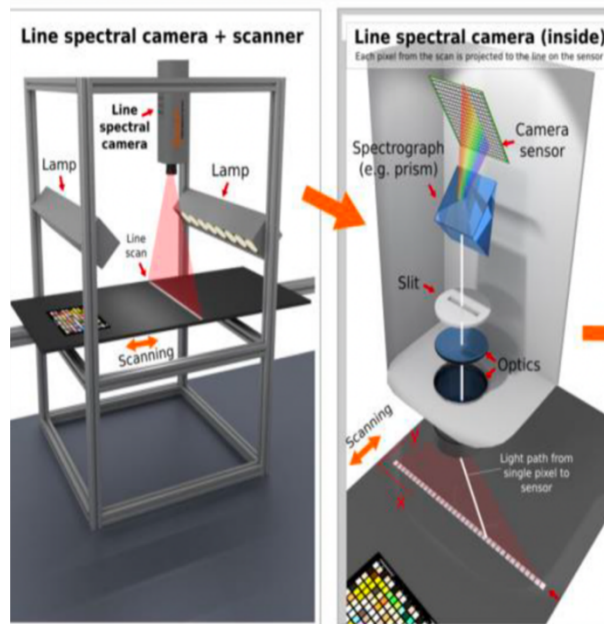


Figure 2: Line scan camera set up and inside camera view.

Both transmittance and reflectance utilize the line-scan hyperspectral imaging method, which acquires spatial and spectral data simultaneously. The application of hyperspectral methodology leads to the creation of a specialized two-dimensional image (y, λ) that effectively amalgamates both spatial and spectral information. This image provides a comprehensive depiction where each pixel represents a distinct spatial location and corresponds to a specific spectral wavelength. By further extending this concept, a complete hypercube (x, y, λ) is meticulously constructed. This construction involves systematically scanning the entire surface of the sample in the designated motion direction (x) , thereby encompassing a wealth of spatial and spectral details. This hypercube encapsulates an intricate data structure wherein each point holds valuable insights into both the spatial arrangement and spectral characteristics of the sample.

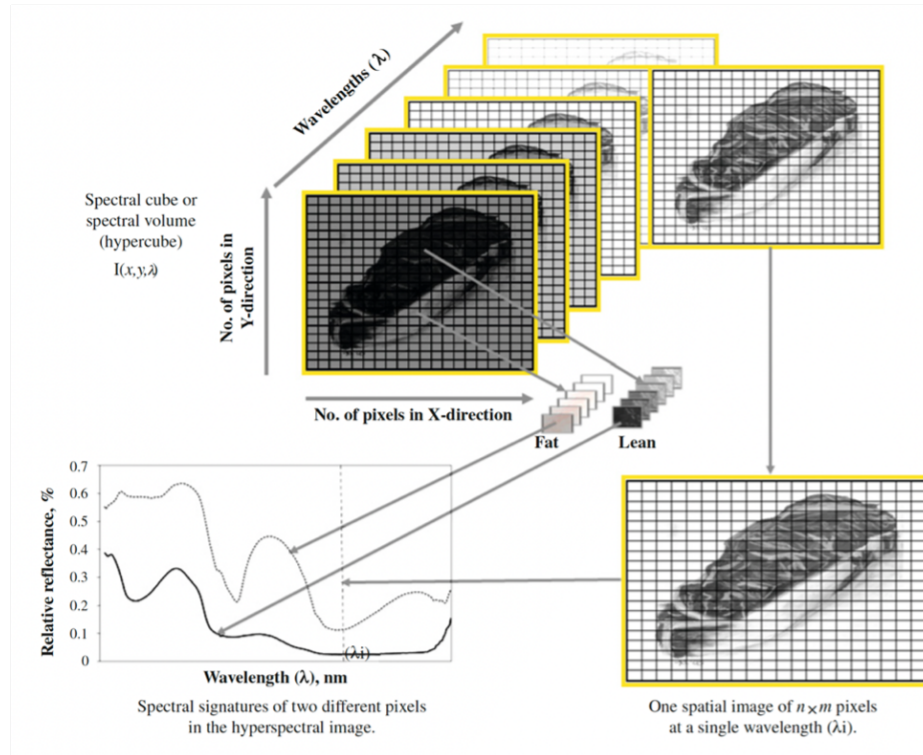


Figure 3: The hyperspectral image (hypercube) of a meat sample demonstrates the spectral-spatial correlation, with each pixel representing a specific spectrum. Figure reprinted from [43].

A hyperspectral data of meat can be seen in figure 3 [43]. It is notable that fat and lean portions of the meat exhibit distinct spectra, as depicted in the accompanying figure 3. This disparity in spectra arises from the inherent differences in their composition and molecular structures. The figure visually demonstrates how the spectral profiles of fat and lean regions within the meat sample vary, allowing for differentiation and characterization of these components.

Each pixel within the hyperspectral image corresponds to a specific spectrum. This means that for every point in the image, detailed spectral information is captured, allowing for precise characterization and analysis. By mapping the spectral information onto the spatial dimensions, the hyperspectral image provides a comprehensive representation of the meat sample, enabling researchers to study and identify various components and characteristics [45].

Line-scan hyperspectral imaging techniques offer a versatile and effective approach for conducting spatially resolved spectroscopy measurements [44].

Employing a single CCD exposure, this methodology concurrently gathers a sequence of spectra across a broad array of offsets, all while preserving a fine spatial interval. The outcome of this process is a scattering image (y, λ) derived from a solitary scan. Within this image, a comprehensive assemblage of spatially resolved spectra is contained, furnishing a substantial reserve of spatial and spectral data. This reservoir of information is pivotal for the in-depth evaluation of subsurface attributes and characteristics.

3.3 Focal plane array (FPA) and Scanning

Focal plane array (FPA) technology is a key component in modern imaging systems, particularly in the field of infrared and thermal imaging. FPAs are two-dimensional arrays of individual light or radiation detectors integrated onto single semiconductor chip. In a focal plane array, each individual detector element, referred to as a pixel, plays a crucial role in capturing incoming light or radiation and subsequently converting it into an electrical signal. These pixels, often constructed on a single semiconductor chip, possess the remarkable capacity to densely populate an array due to their compact nature. This attribute allows for a substantial number of pixels to be intricately arranged, contributing to the overall efficacy of the system. Depending on the application and desired resolution, the size and shape of the pixels can vary. Each pixel contains a detector material that is sensitive to the wavelength or kind of radiation under observation, such as visible light, infrared radiation, or thermal radiation[44].

When light or radiation strikes a pixel, it interacts with the detector material, resulting in a response. This response can take the form of electron-hole pairs being generated in a photon detector, such as a photodiode, or a change in resistance or temperature being caused in a thermal detector, such as a bolometer. The generated electrical signal from each pixel is then typically amplified, digitized, and processed by the readout electronics integrated into the FPA. The combination of signals from all the pixels forms an image or data representation of the captured scene or object.

The use of an array of individual detector elements, or pixels, in an FPA allows for simultaneous detection of light or radiation across the entire field of view, enabling high-resolution imaging[45].

3.4 Hyperspectral camera

A spectral camera, also referred to as a hyperspectral camera, is an imaging instrument designed to gather data from numerous wavelengths or spectral bands. Unlike regular cameras that capture images in just three primary colors (red, green, and blue), spectral cameras have the capability to capture images in numerous narrow spectral bands, ranging from hundreds to thousands. This unique feature allows spectral cameras to collect intricate spectral information about the objects or scenes they capture.

3.4.1 Working principle.

The operational principle of a spectral camera involves the following steps:

3.4.2 Optics

In a hyperspectral camera, the optics have a vital role in collecting and guiding the incoming light onto the detector or sensor. Typically, the optics consist of lenses, mirrors, or a combination of both, depending on the camera's design.

The primary purpose of the optics is to precisely focus the incoming light onto the detector or sensor. This ensures that the captured image is clear and well-defined. The lenses or mirrors within the optics system control the direction and path of the light, minimizing distortions and aberrations that could impact the quality of the spectral image. The specific design and configuration of the optics can vary based on the desired performance and application of the hyperspectral camera. Some cameras may employ specialized optics like telecentric lenses to achieve consistent illumination and image quality throughout the entire field of view. Others may incorporate optical filters or prisms within the optical path to enhance spectral separation and improve the camera's spectral resolution.

3.4.3 Detector

In the realm of spectral cameras, the detector plays an indispensable role in the transformation of incident light into electrical signals. Two widely used detectors in these cameras are charge-coupled devices and complementary metal-oxide-semiconductor sensors.

CCDs have firmly established their position as detectors of choice across diverse imaging applications. They consist of an array of light-sensitive pixels, wherein

incident photons are converted into electrical charge. Each pixel within a CCD accumulates charge in direct proportion to the intensity of the incident light it receives. Subsequently, once the image capture phase concludes, the accumulated charge is systematically read out row by row. The resultant electrical signals are then meticulously processed to reconstruct the complete spectral image.

On the other hand, CMOS sensors have gained prominence owing to their distinct advantages, including reduced power consumption, enhanced readout speeds, and integrated functionalities. Similar to CCDs, CMOS sensors comprise an array of pixels. However, what distinguishes CMOS sensors is that each individual pixel is outfitted with its own dedicated amplifier and readout circuitry. As light reaches a pixel, it triggers the generation of an electrical signal within that very pixel. This inherent design facilitates expedited readout processes and has the potential to diminish noise levels compared to CCDs.

Both CCDs and CMOS sensors perform the fundamental task of converting light into electrical signals. However, they differ in terms of performance, cost, and application-specific requirements. The choice between the two depends on factors such as desired spectral resolution, sensitivity, readout speed, power consumption, and budget considerations[46].

3.4.4 Spectral dispersing element

The Spectral Dispersing Element is an essential component in a spectral camera that separates incoming light into its individual wavelengths. It is commonly achieved using prisms or diffraction gratings.

Prisms use refraction to separate light into its constituent wavelengths. As light passes through a prism, different wavelengths experience varying amounts of refraction. This causes the wavelengths to disperse, spreading them out and enabling their separation. The dispersed light is then directed onto the detector, creating a spectral image.

Diffraction gratings consist of a surface with regularly spaced lines or grooves. When light interacts with a diffraction grating, it undergoes diffraction, resulting in the spreading out of the light waves. This produces a series of spectral orders, with

each order corresponding to a specific wavelength. By capturing different orders of the diffracted light, a spectral image can be obtained.

Both prisms and diffraction gratings offer the ability to separate light into its constituent wavelengths, allowing the acquisition of spectral information. The choice between the two depends on factors such as desired spectral resolution, dispersion efficiency, and specific application requirements.

The Spectral Dispersing Element spreads the light across the detector, enabling the camera to capture a spectral image. This image contains valuable data about the light's intensity at different wavelengths, which can be further processed and analyzed to extract spectral characteristics or identify specific materials based on their unique spectral signatures.

3.4.5 Data acquisition:

Data acquisition in a hyperspectral camera involves the detector capturing the spectral image by recording the light intensity at each pixel across the spectral bands. This enables the camera to obtain a detailed spectral profile of the scene or objects being imaged.

The detector in a hyperspectral camera is an array of pixels, where each pixel corresponds to a specific wavelength. The spectral resolution is contingent upon the quantity of pixels within the detector, where a higher number of pixels correlates to finer and more intricate spectral details.

During data acquisition, the detector measures the light intensity at each pixel across the entire range of spectral bands. The recorded intensity values represent the amount of light energy detected at each wavelength. This information is stored for each pixel, resulting in a two-dimensional image with spatial and spectral coordinates.

By capturing the light intensity at each pixel across the spectral bands, the hyperspectral camera acquires a comprehensive spectral profile of the scene or objects. This enables detailed analysis and characterization of materials and features based on their unique spectral signatures.

After data acquisition, further processing can be performed on the captured spectral image. This may involve calibration, noise reduction, and image correction

techniques to enhance the image quality and extract meaningful spectral information. Subsequently, advanced algorithms can be employed to scrutinize the acquired spectral data, facilitating the identification of particular materials or characteristics through the discernment of their distinct spectral signatures.

3.4.6 Data Processing

Data processing is an essential step in a spectral camera that aims to extract meaningful spectral information from the captured data. Its primary purpose is to enhance the quality of the spectral image and enable analysis and identification of specific materials or features based on their spectral signatures. The data processing stage involves several techniques.

Firstly, calibration corrects for systematic errors and inconsistencies in the spectral data. It compensates for variations in detector response, non-uniformities in illumination, and instrumental artifacts, ensuring accurate and reliable spectral data.

Next, noise reduction techniques are applied to minimize unwanted noise in the spectral image, arising from sources like photon noise, detector noise, and environmental interference. These techniques use filtering algorithms and statistical methods to reduce noise while preserving the integrity of the spectral information.

Image correction techniques are then used to rectify distortions or artifacts in the spectral image. These corrections can compensate for geometric distortions, remove atmospheric effects, or correct spectral smile or wavelength shift caused by the camera system. Image correction ensures an accurate representation of the imaged scene or objects.

Lastly, spectral analysis employs advanced algorithms for extracting meaningful information from the spectral data. This analysis can involve statistical methods, machine learning techniques, or spectral unmixing algorithms. It allows for the identification of specific materials or features based on their spectral signatures and enables quantitative analysis, such as determining substance abundance or concentration in the scene.

Overall, the data processing stage of a spectral camera is crucial for refining and extracting valuable information. It encompasses calibration, noise reduction,

image correction, and advanced algorithms for spectral analysis and identification of materials or features.

3.5 Fourier transform infrared (FTIR) Imaging

In their early stages, focal plane array detectors were primarily developed for military and astronomical applications, serving purposes such as smart missile guidance systems and astronomical imaging devices for observing galaxies. However, the evolution of these detectors has extended their utility to the realm of materials research. Available in array formats such as 64x64 or 128x128 individual elements, these detectors now offer capabilities for capturing thousands of FTIR spectra concurrently from diverse points within a sample. This innovative approach enables the determination of concentration and distribution patterns of specific compounds across the sample's field of view. Consequently, FTIR imaging can aptly be compared to a form of chemical photography [47].

FTIR imaging provides a valuable technique that eliminates the need for dyes and labels, offering a rapid and dependable approach to produce two-dimensional images that improve the visualization of biological, pharmaceutical, and polymeric materials. The focal plane array (FPA) detector demonstrates its versatility in facilitating FTIR imaging, effectively operating in both transmission and attenuated total reflection modes.

3.5.1 Transmission imaging

In the transmission mode of FTIR spectroscopy, infrared light traverses through the sample, and the detector gauges the absorbance. This technique typically yields spectra characterized by a robust signal-to-noise ratio (SNR) due to the ample infrared light intensity reaching the detector. However, the thickness of the sample assumes a pivotal role in this form of measurement.

In order to prevent the complete absorption of infrared energy, it is necessary to shape the sample into a thin film. Maintaining uniform thickness throughout the sample becomes crucial for accurate quantitative analysis. When utilizing the transmission method for imaging a heterogeneous sample, it's important to consider the dimension of the specific domain related to the component of interest when determining the sample's thickness. Ideally, the thickness should either match or be

smaller than the domain's size to ensure that the obtained results carry significant relevance [48].

3.5.2 Attenuated total reflection imaging

Attenuated total reflection (ATR) imaging is an infrared spectroscopy technique used to study the chemical content and distribution of samples. Unlike transmission mode, which involves passing infrared light through the sample, ATR imaging involves monitoring the attenuated reflection of infrared light at the sample interface. ATR imaging entails the contact of a sample with an ATR crystal, typically possessing a high refractive index. The infrared light is directed at a precise angle into the ATR crystal, exceeding the critical angle for total internal reflection. As light engages with the sample at the interface between the crystal and the sample, it undergoes several internal reflections and infiltrates to a specific depth. At each reflection, the infrared light interacts with the sample, and its intensity diminishes in accordance with the chemical composition of the sample. The attenuated light is then detected by a detector, yielding an infrared spectrum. An ATR image can be formed by scanning the sample across the ATR crystal, mapping the chemical distribution across the sample's surface. ATR imaging is a strong technique that combines the benefits of infrared spectroscopy with high spatial resolution, enabling comprehensive chemical mapping of samples without considerable sample preparation.[48].

3.6 FPA-FTIR vs hyperspectral camera

Fourier Transform Infrared (FT-IR) spectroscopy necessitates distinct measurements for individual samples, whereas Focal Plane Array FT-IR (FPA-FT-IR) has the capacity to concurrently scrutinize multiple minute samples. However, the latter method does entail additional time for analyzing microplastics (MPs). The endeavor to broaden the wavenumber spectrum in FT-IR spectroscopy encounters challenges due to the elevated cost associated with employing broadband focal plane arrays (FPAs), often composed of materials such as HgCdTe. These materials mandate cooling mechanisms to achieve the prerequisite low operational temperature, which results in larger equipment dimensions, augmented mass, and escalated costs.

To surmount these obstacles, researchers have adopted hyperspectral cameras that function within constrained wavenumber ranges, particularly in the near-infrared and short-wavelength infrared bands, for microplastics analysis. The SWIR band has proven effective in distinguishing various types of plastics.

Recent advancements have yielded a compact hyperspectral camera designed for the long infrared band. This innovation leverages a microbolometer, an economical uncooled focal plane array (FPA) known for its heightened sensitivity in the LWIR region. Moreover, the camera is furnished with an imaging-type 2D Fourier spectrometer, enabling the evaluation of a cell with a 20 mm diameter within the visible light range.

In contrast with FPA-FT-IR systems, a LWIR-band hyperspectral camera offers superior cost-effectiveness, compactness, and expeditious performance. Its characteristics render it particularly well-suited for the surveillance of black microplastics (MPs), with its portability catering to field studies and applications aboard research vessels.

4 Material and Methods

4.1 Sample preparation

To ensure the attainment of precise and reliable results, meticulous sample preparation procedures were followed. The first step involved the thorough cleaning of each sample to eliminate any potential sources of interference, such as dirt, debris, or residues. This cleaning process aimed to provide a pristine surface for accurate spectral measurements, minimizing any external influences on the analysis.

Subsequently, sections from each sample were carefully selected, taking into account factors such as color, texture, and overall condition. These sections were chosen with the utmost care to faithfully represent the specific properties of the black plastic materials under investigation. The samples employed in this study encompassed a diverse range, including Pepsi, shaving gel, tennis ball box, knife, tomato ketchup clothing hanger, biscuit box, food container, washing gel box, USB data cable, cleaning brush, meat container, garbage bag, and PVC tape, as illustrated in the accompanying figure 4. Each sample was assigned a unique numerical identifier, ranging from 1 to 15, as clearly depicted in the figure 4.

In order to obtain microplastics or plastic powder, a metal work file with a diameter of approximately 200 mm, as shown in the figure 5, was utilized. For samples 1 to 10, which consisted of hard plastics, the metal file was employed to grind them into micro-sized particles. This process involved carefully manipulating the samples against the file's surface to achieve the desired size reduction. The use of the metal file ensured consistency and uniformity in the production of micro-sized particles, enabling accurate spectral measurements.

Following the grinding process, the resulting microplastics or plastic powder were utilized for further analysis. The micro-sized particles provided valuable insights into the spectral properties of the hard plastic samples. Conversely, due to the inherent softness of samples 11 to 15, they could not be effectively ground into micro-sized particles using the metal file. As a result, these samples were exclusively used for macro-scale measurements, contributing to a comprehensive understanding of the behavior of soft plastic materials under investigation. The careful selection and preparation of the samples, along with the distinction between hard and soft plastics,

allowed for a systematic analysis of the spectral properties of the black plastic samples.



Figure 4: 1) Pepsi lid, 2) shaving gel lid, 3) tennis ball box lid, 4) knife, 5) tomato ketchup lid, 6) clothing hanger, 7) biscuit box, 8) food container, 9) washing gel box, 10) Coca Cola lid, 11) USB data cable, 12) cleaning brush, 13) meat container, 14) garbage bag, and 15) PVC tape.



Figure 5: Metal work file round 200 mm used to make micro plastics.

4.2 Methods

4.2.1 Point scan measurement

In point scan measurements, only a single spectrum can be obtained from a sample of black plastics. To conduct point scan measurements in air, the samples are cut into approximately $2 \times 2 \text{ cm}^2$ using scissors, ensuring that all samples have flat surfaces, which is crucial for achieving accurate results. Both hard and soft samples are utilized in air for point scan measurements in order to obtain reflectance spectra. The wavelength range used for these measurements are from 250 nm to 2500 nm. Prior to initiating the point scan measurements, the system was calibrated. Each reflectance point measurement typically required around 3 to 4 minutes to complete. The resulting data is saved in CSV files and subsequently analyzed using Python programming language.

For the analysis of microplastics, bulk microplastic samples (BMPs) were carefully prepared to conduct point scan measurements (PSM). The hard plastics were ground down to micro-sized particles, enabling their examination through PSM. However, soft plastics such as meat containers, garbage bags, and PVC tapes were unsuitable for grinding into micro-sized particles due to their inherent characteristics.

To facilitate the measurements, a cuvette was employed, as illustrated in the accompanying figure 6. The cuvette served as a vessel to mix water with the black microplastics. Significantly, owing to the reduced density of the BMPs, they exhibited a tendency to remain afloat on the water's surface. To tackle this concern, the cuvette underwent vigorous shaking, leading certain microplastics to submerge into the water. Over time, these submerged microplastics would gradually resurface. This behavior is observable in the figure 6, where the bottom part of the cuvette displays microplastics immersed in the water, while the majority of them remain on the water's surface. The point scan beam passes through the middle of the cuvette, enabling measurements to be taken at an optimal location.



Figure 6: Cuvette with water and microplastics

In conducting the measurements, transmittance point scanning was employed. Each measurement required approximately 1 to 2 minutes to complete, providing ample time to obtain accurate readings before the BMPs floated to the surface. The process involved starting with the minimum quantity of BMPs (samples) and thoroughly shaking the cuvette to ensure proper dispersion. Measurements were then taken, followed by the addition of small increments of BMPs and subsequent shaking. This stepwise procedure was repeated using five different quantities, progressing from minimum to maximum. Although the specific weights of the quantities were not determined, their relative proportions were maintained throughout the measurements.

The transmittance of both water and BMPs in water was measured using point scanning. The resulting data, comprising the transmittance values at different wavelengths, was recorded and saved in CSV files. Subsequently, these data files were subjected to comprehensive analysis utilizing the Python programming language, enabling the extraction of valuable insights and information regarding the characteristics of the microplastics under investigation.

4.2.2 Hyperspectral imaging

For the precise hyperspectral imaging of black microplastics (BMP), a carefully designed experimental setup was utilized, as depicted in the accompanying figure 7. A spectral camera operating within the 400 to 1000 nm wavelength range was employed to detect and analyze the BMPs present in water. The hyperspectral camera was positioned in a vertical orientation, ensuring proper alignment with both the scanner and the samples under investigation. By synchronizing the hyperspectral camera and the scanner, and connecting them to a computer, precise control and coordination of the imaging process were achieved. The computer interface facilitated the adjustment of the scanner's position and rotation according to the specific requirements of the experiment, allowing for optimal imaging conditions.

To accurately determine the transmittance and reflectance of BMPs in water, a calibration process involving white and black references was employed. The initial step involved measuring the reflectance of black macro plastics in air as a baseline reference before transitioning to the analysis of black microplastics. To capture the spectral data, a plate was used instead of the cuvette typically employed in point scan measurements. The plate was filled with a controlled amount of tap water, as illustrated in the figure, providing a suitable medium for the measurements. Reflectance measurements were performed using a black reference, while transmittance measurements utilized a white reference.

To systematically assess the spectral properties, a methodical approach was adopted. Initially, only water was present in the plate, allowing for the determination of the transmittance and reflectance of water alone. Subsequently, small quantities of black microplastics were incrementally added to the plate, followed by the introduction of additional small quantities. This stepwise procedure enabled the evaluation of three different quantities of black microplastics, facilitating a comprehensive analysis of their transmittance and reflectance characteristics.

The hyperspectral camera utilized in the imaging process generated a substantial amount of data during each measurement, resulting in a significant dataset for analysis. It is noteworthy that a single measurement could yield data files of approximately 1GB in size. To ensure the accuracy and reliability of the acquired

hyperspectral data, sophisticated Python code was employed for data correction, compensating for any instrumental artifacts or noise present in the measurements. Furthermore, the extensive dataset was subjected to in-depth analysis using advanced Python programming, allowing for the extraction of valuable insights and meaningful conclusions regarding the spectral characteristics and behavior of the black microplastics under investigation.

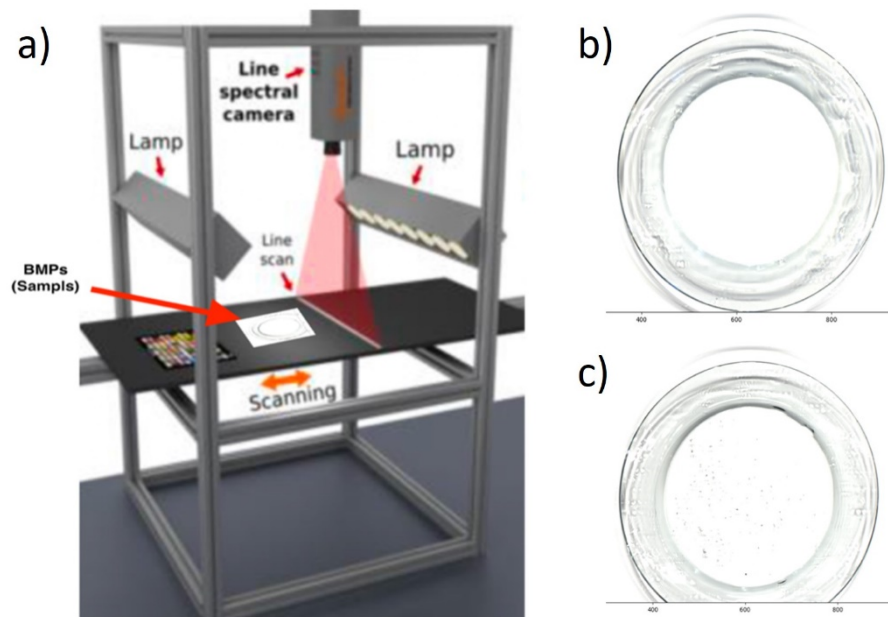


Figure 7: a) Hyperspectral imaging set b) Plate with water c) Plate with water and black microplastics.

5 Results and discussion

Both the point scanning and hyperspectral imaging methods have been utilized in this study. In the following sections, we will discuss the results obtained by these two methods separately to highlight their respective contributions to the analysis.

5.1 Point scanning

5.1.1 Black macro plastics in air

Before digging into the analysis of microplastics in water, it is essential to first discuss macro plastics in air using the point scan method. This approach allows for a focused examination of larger plastic particles and serves as a comparative reference for subsequent microplastics analysis. However, it is worth noting that the point scan method presents certain challenges due to the small spot size of the beam, which makes it difficult to select specific areas of interest because it might not cover a wide enough area for comprehensive analysis. Nevertheless, it is considered more accurate than HSI in capturing detailed reflectance information.

To study macro plastics, black plastic samples measuring $2 \times 2 \text{ cm}^2$ were carefully arranged for analysis. Reflectance measurements were performed using a black reference, serving as a baseline measurement. Initially, measurements were taken with only the black reference in place, followed by the placement of black macro plastics samples to capture the reflectance data. Data was collected separately for the reference and the black macro plastics samples, allowing for comparative analysis.

The collected data, both original and normalized, was processed using Python code and visualized in the figure 8. Considering all the samples together, the maximum reflectance observed for black macro plastics ranged from the ultraviolet to the infrared regions, reaching approximately 18% as depicted in figure 8. However, within specific wavelength ranges, variations in reflectance were observed. For instance, in the range of 2000 nm to 2500 nm, a maximum peak at 11.6% was identified which correspond to spray lid green spectrum. The spray lid sample have most bright surface as compared to the other studied samples. Similarly, within the 1000 nm to 2000 nm range, the maximum reflectance reaches approximately 13.4% and in the 400 nm to 1000 nm range, the maximum reflectance is 18.8% at about 500

nm wavelength. In the UV region, the maximum reflectance was found to be approximately 13% and remains stable from 325 nm to 350 nm and suddenly drops to 7% from 351 nm to 380 nm and then comes to 13% again at 380nm and this behavior is observed for all samples.

Upon closer examination of individual sample spectra, it becomes evident that each sample possesses a distinct reflectance percentage and exhibits a unique spectral behavior. The normalized figure 9 provides a clear depiction of these differences among the samples. For instance, the washing box sample displays a notably different behavior compared to other samples, appearing blackish-blue after the grinding process to produce microplastics. The spray lid, for its shiny surface, exhibits higher reflectance compared to other samples. Conversely, the PVC tape and clothing hanger samples demonstrate lower reflectance spectra compared to the rest of the samples. It is noteworthy that between the wavelength range of 1800 nm and 2270 nm, all samples exhibit more discernible distinctions, suggesting potential variations in their chemical composition or structural properties within this specific range.

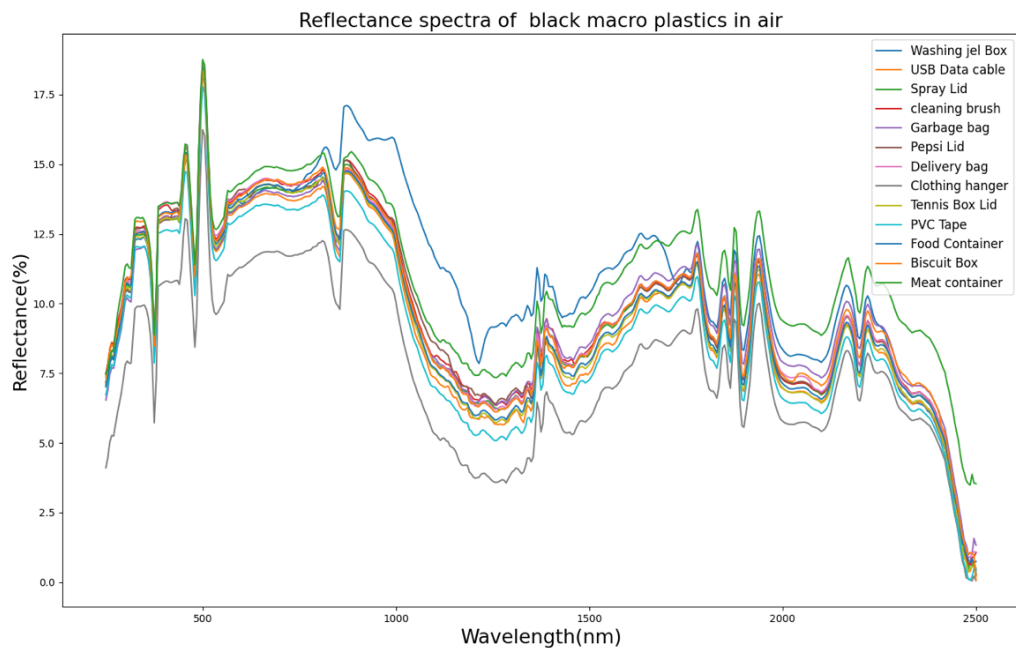


Figure 8: Reflectance spectra of different black macro plastics in air

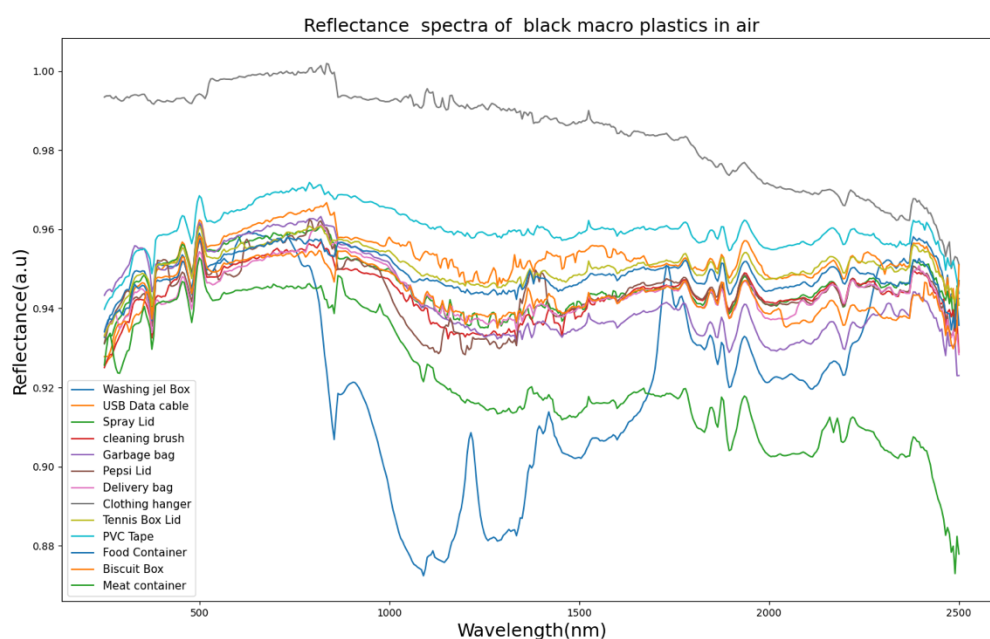


Figure 9: Normalization of Reflectance spectra of different black macro plastics in air

5.1.2 Black micro plastics in water

The objective of this study was to examine the transmittance properties of black microplastic samples at different wavelengths. A selection of black microplastics commonly encountered in daily life was chosen for analysis, including a spray lid, Coca Cola lid, clothing hanger, tennis ball box lid, tomato ketchup lid, food container box, knife handle, washing gel box, and biscuit box. These samples were subjected to transmittance measurements, and the obtained data was utilized to generate a comprehensive understanding of their optical behavior.

To begin the analysis, the transmittance of each black microplastic sample was measured across a wide wavelength range, spanning from 250 nm to 2500 nm. The resulting transmittance spectra were then plotted. This graphical representation provided an overview of the transmission characteristics of the black microplastics under investigation. In order to facilitate a more detailed comparison and interpretation of the data, the transmittance values were normalized. The normalization process enabled a direct comparison between different samples and wavelengths, allowing for a more precise analysis of the transmittance patterns exhibited by the black microplastics. The normalized transmittance values were also depicted in the figure for comprehensive visualization.

It is known that water exhibits varying absorption bands across the studied wavelength range, with absorption being influenced by factors such as temperature. In the visible range, water has minimal absorption, while at longer wavelengths, it becomes absorption increases [56]. Previous research has also demonstrated differences in absorption properties between light water (H_2O) and heavy water (D_2O) [57]. For the current investigation, tap water sourced from the University of Eastern Finland (Joensuu) was used for all measurements, including both point scanning and hyperspectral imaging. The primary objective of this study was to detect microplastics in water.

Initially, measurements were conducted with a cuvette filled with tap water, and the results are depicted in the figure. When the beam was blocked, no signal was obtained, as shown by the red line in figure 10. However, when the cuvette filled with water was removed, allowing the beam to pass unobstructed, a blue spectrum was observed, as illustrated in the figure 10. This blue spectrum covered a wide wavelength range, spanning from UV to visible and IR regions, providing comprehensive coverage across the electromagnetic spectrum.

Subsequently, measurements were taken after placing the cuvette filled with tap water, and the results are presented in the figure. The orange spectrum represents the transmittance of water. It can be observed that water exhibits maximum transmittance in the visible range. However, in the range from 1400 nm to 2500 nm, the transmittance decreases significantly, indicating strong absorption by water, as depicted in the figure 10. When a small amount of black microplastics was introduced into the water, it was observed that the transmittance (green spectrum) was lower compared to that of pure water, suggesting the presence of something within the water sample.

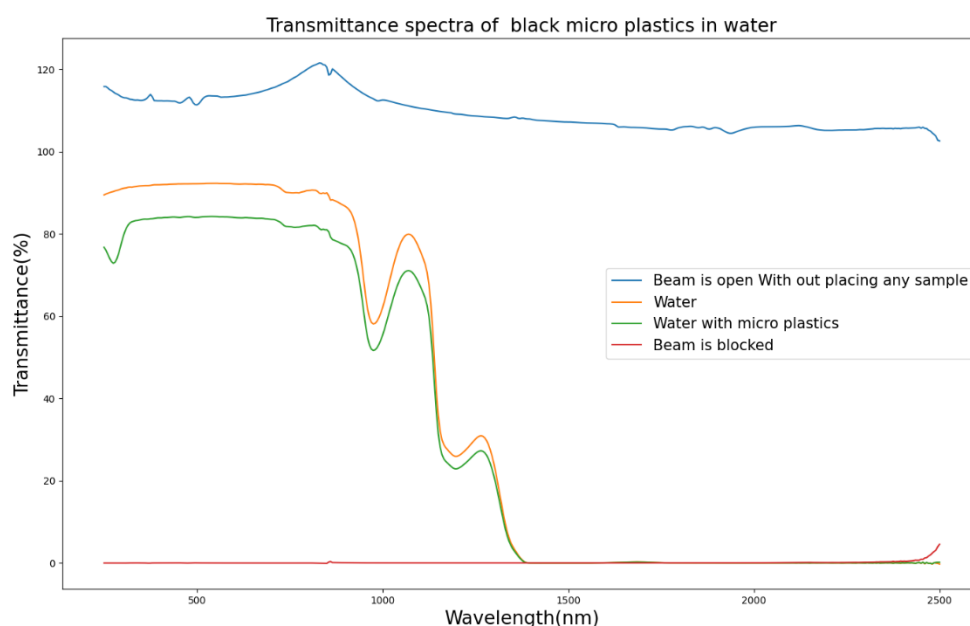


Figure 10: Transmittance of BMPs with and without water.

To isolate the contribution of black microplastics in the overall transmittance, measurements of water transmittance were conducted both with and without the presence of black microplastics. By subtracting the transmittance of water without black microplastics from the overall transmittance data, the isolated transmittance of the black microplastics was obtained. This isolated transmittance curve, displayed in the figures 11 and 12, provided insight into the specific transmittance behavior attributed solely to the black microplastics.

Upon closer examination of the transmittance spectra, it was evident that each black microplastic sample exhibited a unique spectral profile. Notably, variations in peak intensities were observed across the ultraviolet (UV), visible, and infrared (IR) regions. However, in the wavelength range of 1400nm to 2500nm, the transmittance was significantly diminished due to the strong absorption characteristics of water. Consequently, identification or detection of black microplastics within this particular region was challenging.

Within the UV, visible, and near IR regions, the transmittance behavior of the black microplastic samples became more discernible. The figure clearly illustrated distinct peaks at 1270nm and 1070nm, which were accompanied by abrupt changes in the transmittance spectra. In the visible range spanning from 400nm to 800nm, the transmittance profiles of all samples remained relatively constant. However, it is important to note that the actual transmittance values varied among the samples due to differences in the quantities of black microplastics present.

Of particular interest were the distinctive characteristics exhibited by the ketchup lid, food container box, and spray lid samples. These specific samples displayed unique behavior, potentially attributable to variations in the quantity or distribution of black microplastics within each sample. Further investigation into these differences may provide valuable insights into the factors influencing the optical properties of black microplastics.

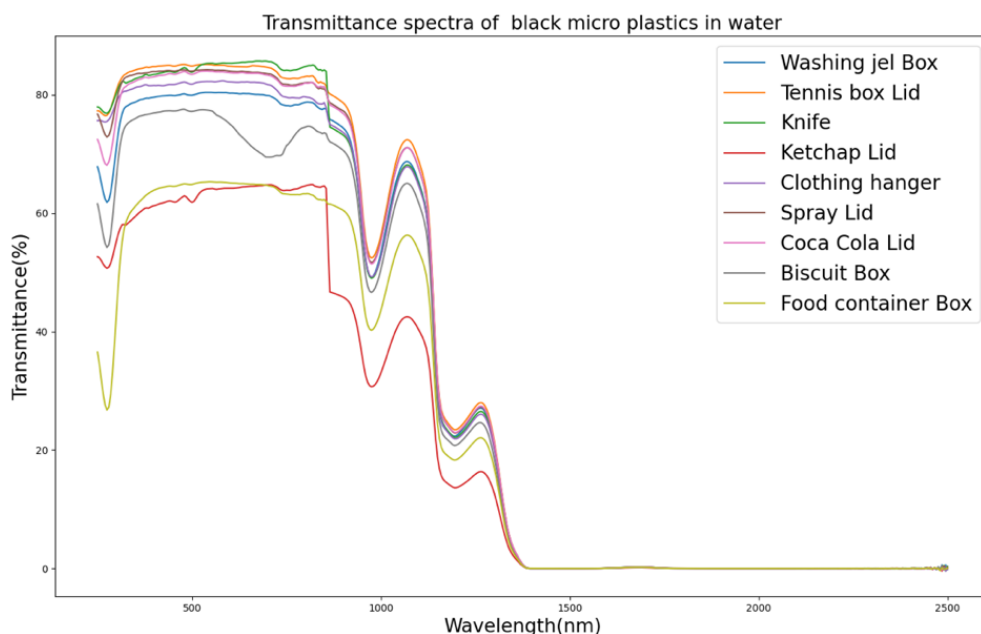


Figure 11: Transmittance spectra of black micro plastics in water

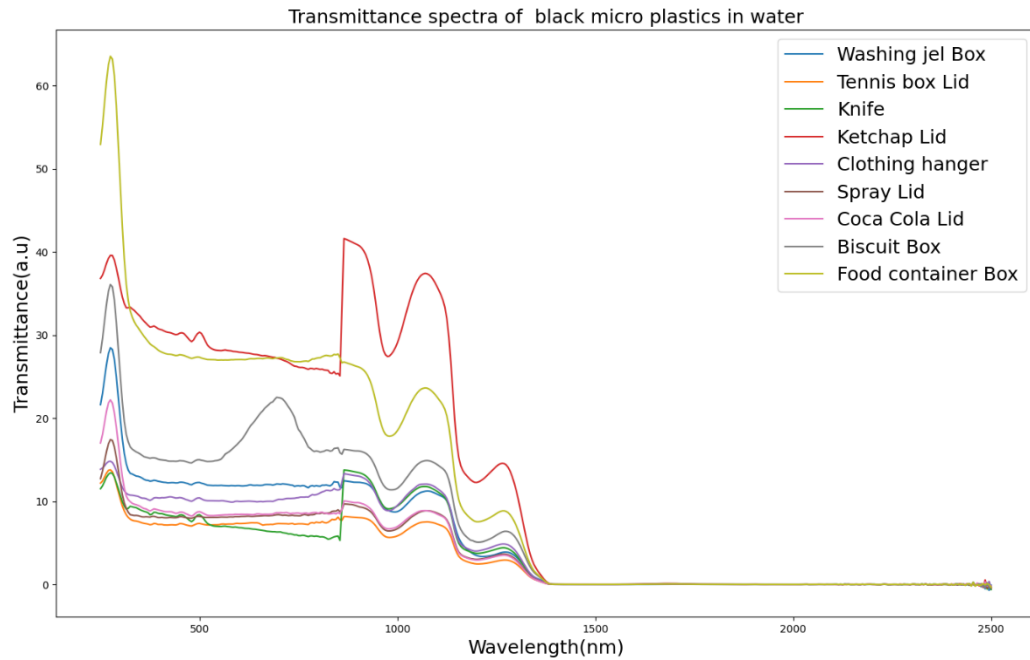


Figure 12: Normalization of Transmittance spectra of black micro plastics in water.

5.1.2.1 Quantity-dependent Transmittance of Black Microplastics in Water

To thoroughly investigate the influence of quantity on the transmittance characteristics of black microplastics (BMPs) in water, a series of five distinct quantities were examined in this study. Each sample initially contained the minimum amount of BMPs, designated as 1 in figure 13. Subsequently, incremental additions of BMPs were introduced to the initial quantity, with subsequent quantities represented as 2, 3, 4, and the maximum quantity as 5 in figure 13.

To gain a thorough comprehension of how quantity affects transmittance characteristics, the measurements were conducted across a spectrum of quantities for the BMPs. Each sample was carefully prepared with a specific quantity of BMPs, and the transmittance values were recorded. The original transmittance data provided insight into the direct relationship between quantity and transmittance.

Both the original and normalized transmittance data were then plotted in the figures, providing a visual representation of the findings. These figures effectively capture the transmittance characteristics of the BMP samples with different quantities, enabling a clear comparison of their respective transmittance profiles. The

figures serve as valuable tools for visual analysis and facilitate a comprehensive evaluation of the influence of quantity on transmittance.

Overall, the inclusion of original and normalized transmittance data, visualized in the figures, enhances the clarity and scientific rigor of the study. These figures enable researchers to directly observe and interpret the relationship between quantity and transmittance for the BMP samples, contributing to a deeper understanding of the optical properties of microplastics and their potential environmental implications.

The primary objective of incorporating varying quantities of BMPs was to establish and analyze the relationship between quantity and transmittance. As the quantities of BMPs increased, a corresponding gradual decrease in transmittance was observed. This clear trend was evident in the figure, where the transmittance values exhibited a progressive decline with each successive increase in BMP quantity. Notably, the maximum quantity of BMPs demonstrated the lowest transmittance among all the samples, which was strikingly illustrated in the figure.

To gain further insights into the impact of quantity on transmittance behavior, the transmittance values were normalized, as depicted in the figure. Normalization facilitated a comprehensive comparative analysis of the transmittance data across the different quantities, enabling a more precise assessment while accounting for potential variations in experimental conditions.

The results of this investigation unequivocally indicated that an increase in the quantity of BMPs led to a corresponding decrease in transmittance. This finding suggests that as the number of BMPs increased within the water sample, there was a higher degree of light absorption or scattering by these particles, resulting in diminished transmittance. The maximum BMP quantity, represented as 5 in the figure, exhibited the least transmittance, implying a significant level of light attenuation due to the larger number of BMPs present.

The outcomes of this study underscore the critical role of quantity in assessing the transmittance characteristics of BMPs in water. Understanding the quantity-dependent behavior provides essential insights into the optical properties and potential environmental impacts of microplastic pollution. This knowledge

contributes to our broader comprehension of the dynamics and behavior of microplastics in aquatic environments and aids in developing effective strategies for their detection and mitigation.

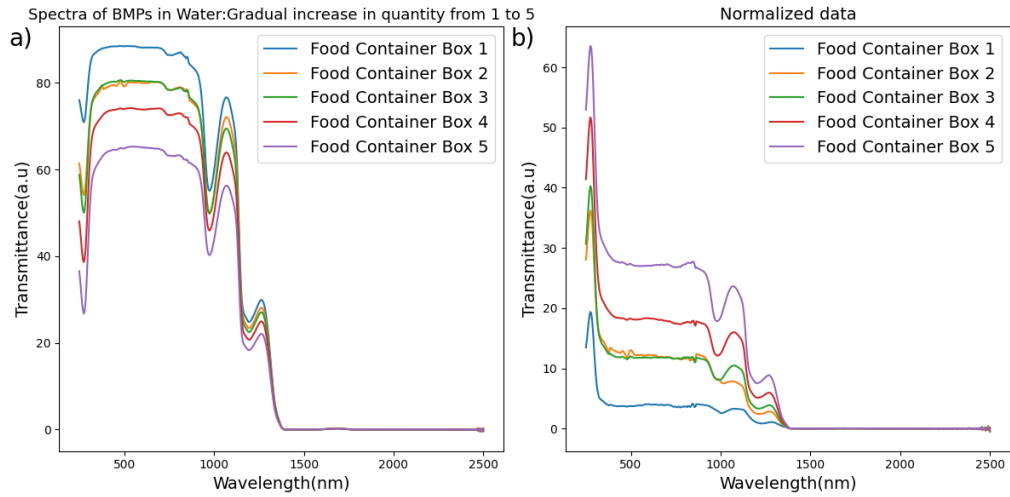


Figure 13: a) Transmittance of BMPs (Food container) in water with vary quantity. b) Normalized data of Transmittance of BMPs (Food container) in water with vary quantity.

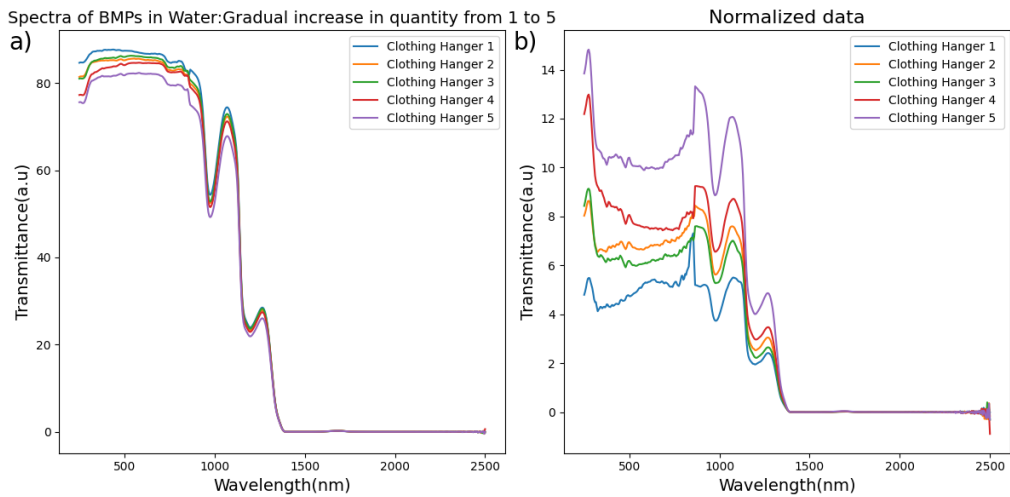


Figure 14: a) Transmittance of BMPs (Clothing hanger) in water with varying quantity. b) Normalized data of Transmittance of BMPs (Clothing hanger) in water with varying quantity.

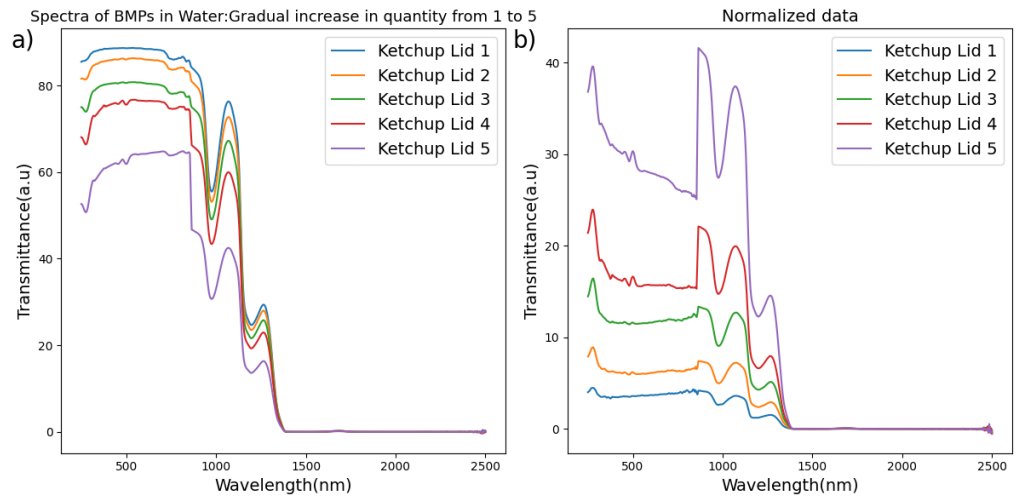


Figure 15: a) Transmittance of BMPs (Ketchup Lid) in water with varying quantity. b) Normalized data of Transmittance of BMPs (Ketchup Lid) in water with varying quantity.

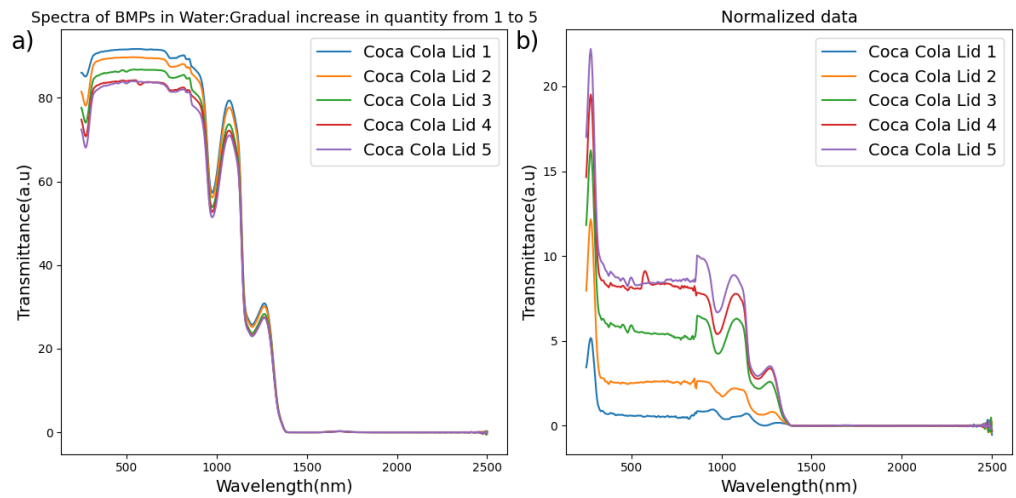


Figure 16: a) Transmittance of BMPs (Coca Cola Lid) in water with varying quantity. b) Normalized data of Transmittance of BMPs (Coca Cola Lid) in water with varying quantity.

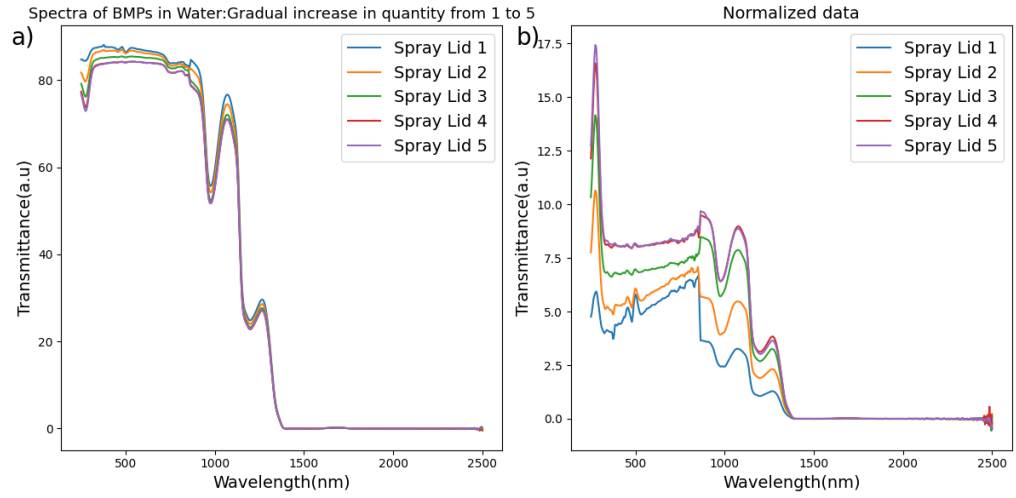


Figure 17: a) Transmittance of BMPs (Spray Lid) in water with varying quantity. b) Normalized data of Transmittance of BMPs (Spray Lid) in water with varying quantity.

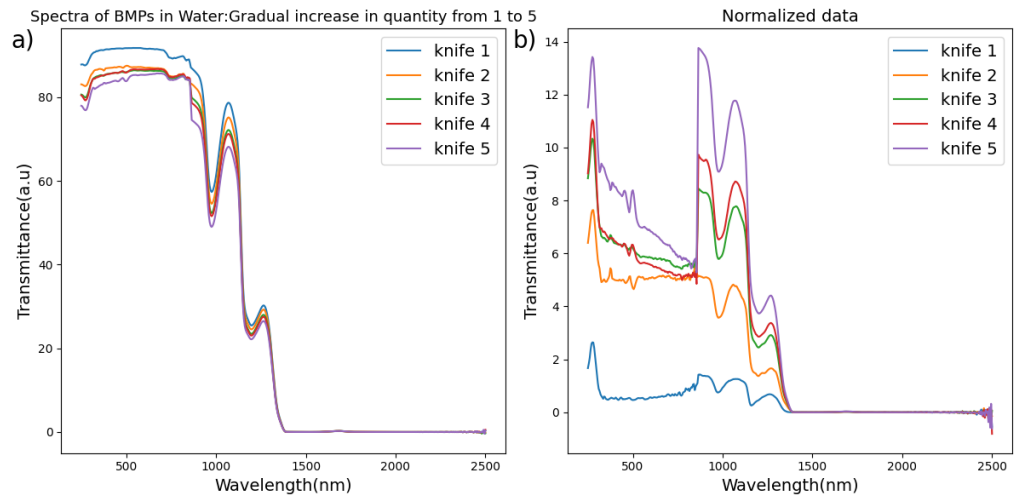


Figure 18: a) Transmittance of BMPs (Knife) in water with varying quantity. b) Normalized data of Transmittance of BMPs (Knife) in water with varying quantity.

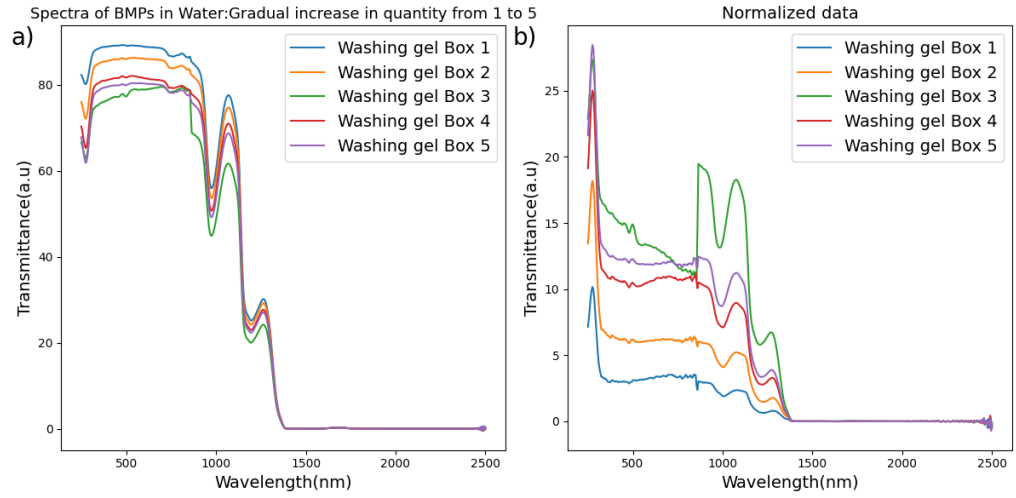


Figure 19: a) Transmittance of BMPs (Washing gel Box) in water with varying quantity. b) Normalized data of Transmittance of BMPs (Washing gel Box) in water with varying quantity.

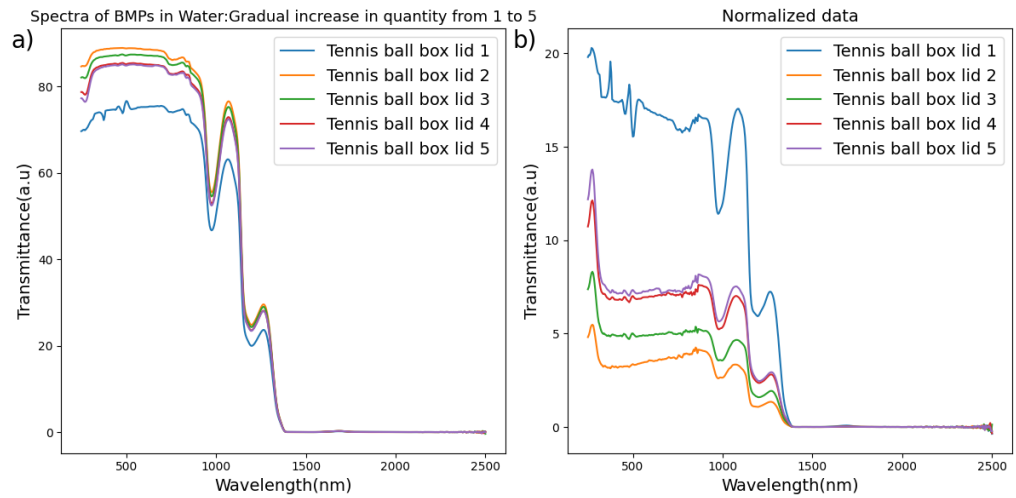


Figure 20: a) Transmittance of BMPs (Tennis box Lid) in water with varying quantity. b) Normalized data of Transmittance of BMPs (Tennis box Lid) in water with varying quantity.

5.2 Hyperspectral Imaging

Transmittance and reflectance results of black microplastic in air will first be discussed and then we will draw some conclusions out of the measurements done with BMPs in water.

5.2.1 Hyperspectral imaging of black macro plastic in air

In this study, we delve into the application of hyperspectral imaging for the detection and analysis of black macro plastic particles suspended in the air. These macro plastic particles are representative of commonly used plastics found in daily life. The aim is to investigate their reflectance properties using a hyperspectral imaging approach. Additionally, we also examine the reflectance and transmittance properties of microplastics, considering various quantities.

To conduct the analysis, we employed two spectral cameras capable of capturing a wide range of wavelengths. The first camera covered the spectral range from 400 nm to 1000 nm, while the second camera extended from 1000 nm to 2500 nm. However, for the purpose of our measurements, we focused on utilizing the spectral camera covering the range from 400 nm to 1000 nm. This allowed us to obtain accurate measurements of reflectance and transmittance for the black macro plastic particles in both air and water environments.

The hyperspectral camera captured detailed images of the black plastic samples under investigation, which can be observed in the accompanying figure 21. To ensure a comprehensive analysis, we selected a total of 13 samples with varying sizes and shapes. These samples were carefully prepared and positioned for reflectance measurements. The objective was to determine the unique spectral properties exhibited by each sample.

To calculate the average spectrum for each sample, we employed the Python programming language. Initially, a square area was carefully chosen for each sample, ensuring that it represented a representative portion of the entire sample's surface. This approach allowed us to obtain a more comprehensive understanding of the reflectance properties across the entire sample.

In contrast to traditional point measurements, hyperspectral imaging provided us with a wealth of spectral information. Instead of capturing a single point spectrum, hyperspectral imaging enabled us to obtain numerous spectra for each sample. By averaging these spectra, we could obtain a more accurate representation of the overall spectral characteristics of each sample. This approach facilitated the

scanning of the entire sample's spectral range and allowed us to selectively examine specific regions of interest.

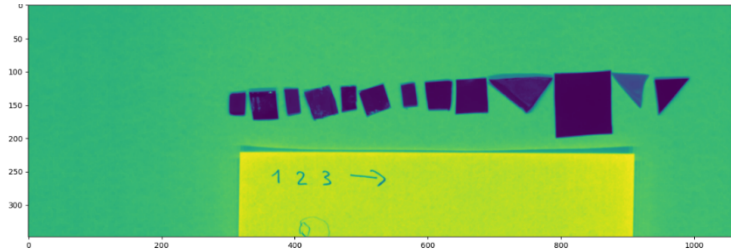


Figure 21: Picture captured by hyperspectral camera of black macro plastics samples.

The process involved plotting the average spectrum of each individual sample alongside the spectra of all other samples, a representation showcased in Figure 22. The two components of Figure 22, namely Figure 22a and Figure 22b, provide essential insights into the reflectance behaviors of distinct macro plastics when exposed to air and subjected to hyperspectral imaging (HSI) analysis.

In Figure 22a, a significant observation arises: the reflectance spectra of all examined samples exhibit minimal values within the visible range of 400nm to 700nm. This tendency undergoes a substantial transformation upon transitioning to the near-infrared (NIR) range around 900nm, where the reflectance reaches its peak value. This transition across the electromagnetic spectrum highlights a considerable shift in reflectance characteristics between the visible and NIR domains. Figure 22b offers a more detailed perspective, revealing that each sample uniquely exhibits variations in reflectance levels when compared to the broader set of samples. This distinctiveness underscores the disparate optical properties inherent to each individual sample. Notably, some samples exhibit a propensity to reflect more light, while others display a diminished reflective behavior, possibly indicating differences in surface shininess or overall reflectivity.

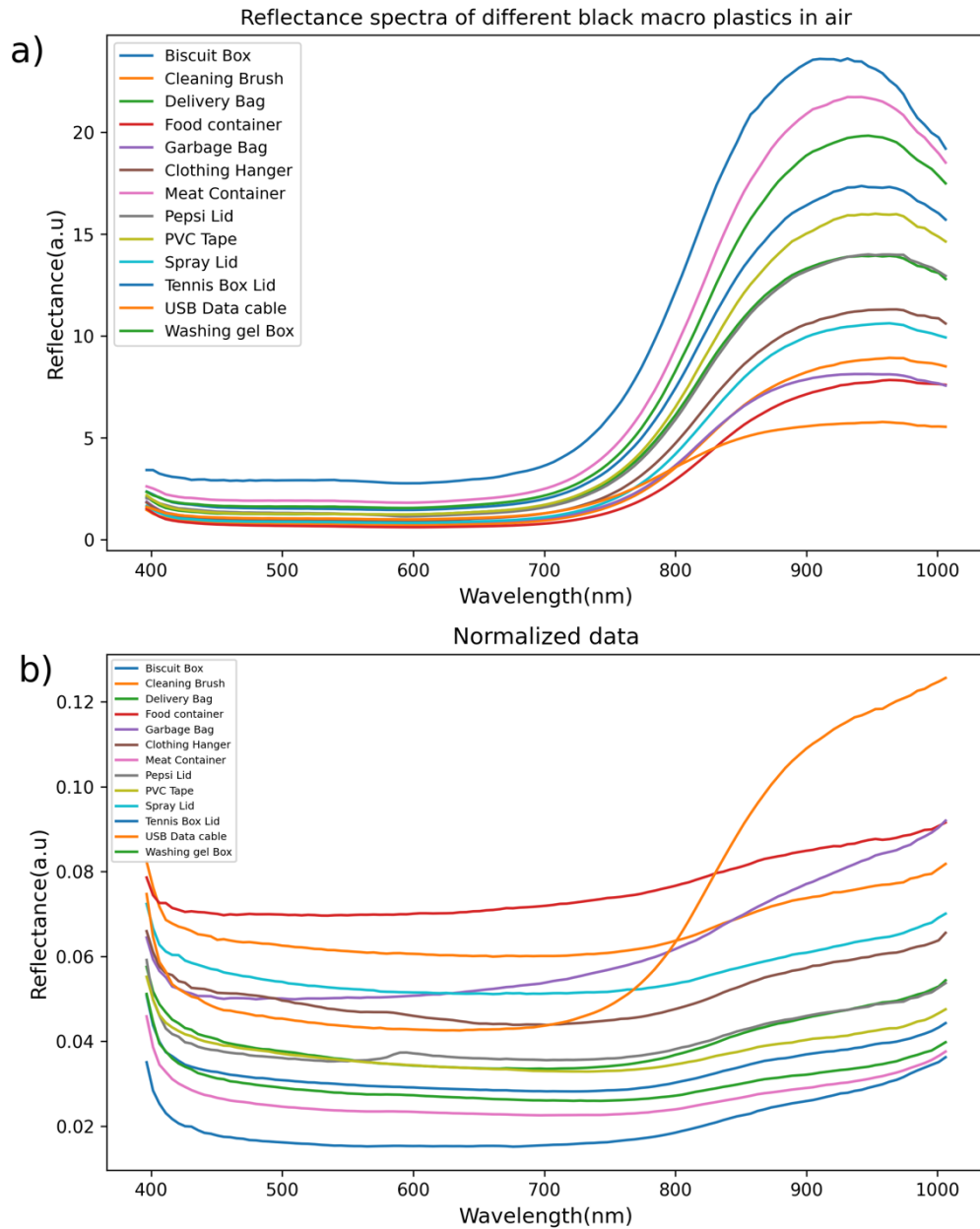


Figure 22: a) Reflectance spectra of different macro plastics in air, b) Normalization of reflectance spectra of different macro plastics in air.

5.2.2 Hyperspectral imaging of black microplastic in water

The discussion encompasses two specific scenarios relating to the reflectance and transmittance properties of black microplastics in water. It begins by examining the transmittance characteristics followed by an exploration of the reflectance properties.

5.2.2.1 Transmittance

To initiate the analysis, the first step involved determining the transmittance of water alone. The average spectrum was then calculated for a specific region of interest within the water contained in the plate. This region was carefully selected, ensuring that it represented a representative area for analysis. The resulting average spectrum, representing the entire green area within figure 23a, was plotted and seen figure 23b for easy reference and examination. Notably, the transmittance value obtained for water was found to be 1.0954 on the y-axis.

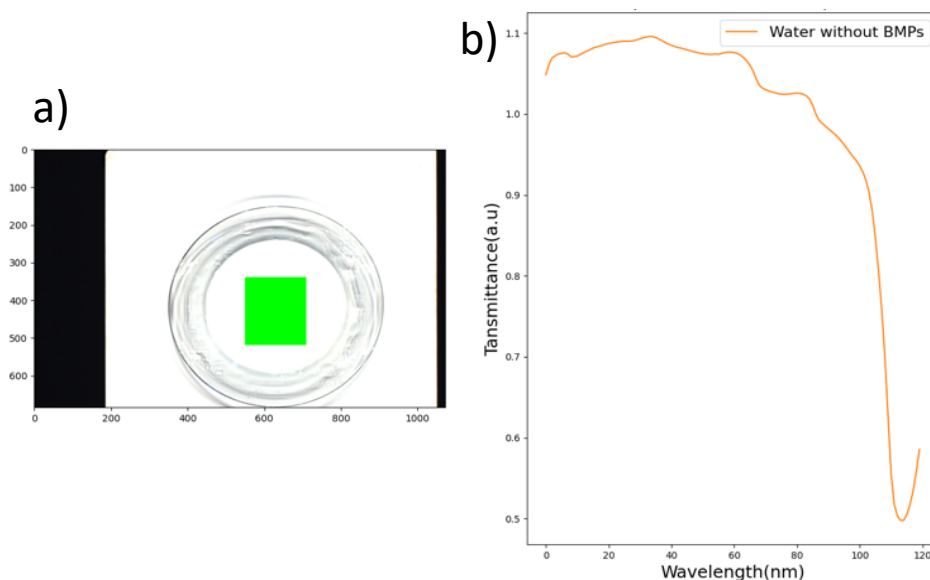


Figure 23: a) Transmittance of water under green area is calculated b) Transmittance spectrum of water without black microplastics.

Subsequently, the investigation proceeded by introducing various quantities of black microplastics into the water sample. The purpose was to assess the impact of these microplastics on the transmittance properties of the water. Following the addition of the microplastics, the average spectrum was recalculated for the desired area within the plate. This area was carefully selected to accurately represent the region of interest. Additionally, for comparison and reference, the average spectrum of the area outside the plate region was also determined.

To ensure the accuracy and reliability of the findings, both the inside and outside plate spectra were plotted and presented in the figure 24. The results showed

that the peak transmittance value inside the plate was measured at 1.074, while the outside plate exhibited a slightly higher peak transmittance value of 1.078. Although the difference between these values is relatively small, it is still discernible. These findings suggest that the presence of black microplastics in the water has a subtle but noticeable effect on the transmittance properties.

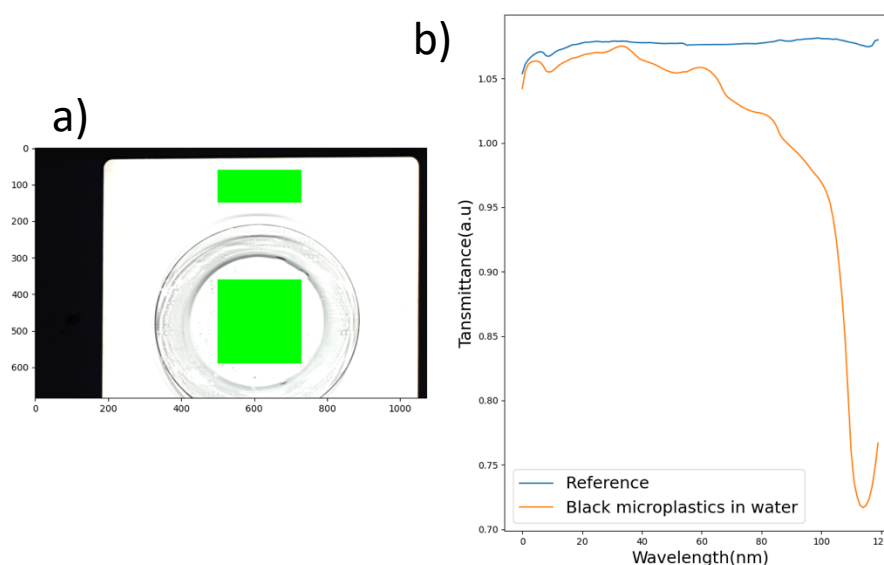


Figure 24 a) Transmittance of water with BMPs and reference green area outside plate. b) Transmittance spectra of water with black microplastics and reference.

Interestingly, when comparing the transmittance of water alone (with a peak value of 1.095) to the transmittance of water with the addition of a small quantity of microplastics (with a peak value of 1.074), a distinct decrease in transmittance becomes apparent. This reduction in transmittance implies the presence of light-absorbing substances within the water, resulting in a decreased overall transmittance value.

The analysis described above was performed for each of the nine samples, ensuring a comprehensive evaluation of the transmittance properties of black microplastics in water. The resulting data from all samples were then combined and plotted together to provide a holistic view and facilitate a comparative analysis of the transmittance characteristics observed across the different samples.

Figure 25 clearly demonstrates the distinct transmittance spectra exhibited by each sample. Notably, the washing gel box sample stands out due to its unique behavior compared to the other samples. This divergence in behavior can be attributed to the fact that when the washing gel box was ground into microplastics, it displayed a bluish-black color. Consequently, the resulting spectra of this sample exhibit noticeable deviations from the other samples.

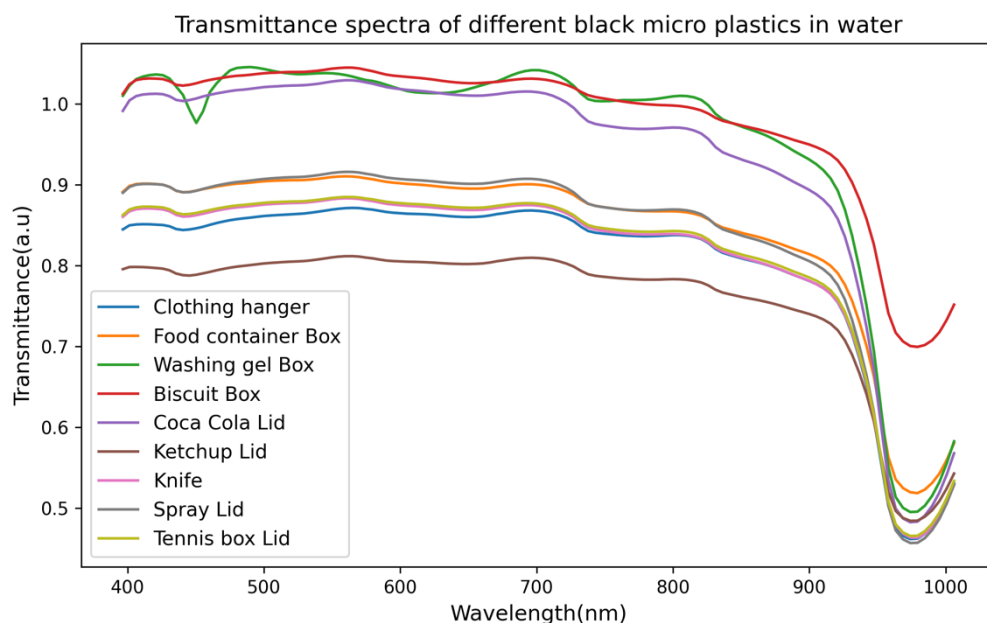


Figure 25: Transmittance spectra of different black micro plastics in water.

Moreover, an abrupt change in transmittance can be observed in the spectral range from 900 nm to 1000 nm. Within this range, the transmittance values undergo a significant shift. Specifically, the peak transmittance values are observed to be around 1.0 in the spectral range from 400 nm to 900 nm. However, beyond 900 nm, the transmittance values drop to approximately half, reaching a value of 0.5. This abrupt change in transmittance behavior may be attributed to the specific interactions between water and the material being analyzed, leading to distinct properties within this spectral range.

Overall, the transmittance spectra of the different samples highlight the variability in the optical behavior of black microplastics in water. The unique characteristics exhibited by each sample underscore the importance of understanding

the specific properties and composition of microplastics to accurately interpret their transmittance spectra.

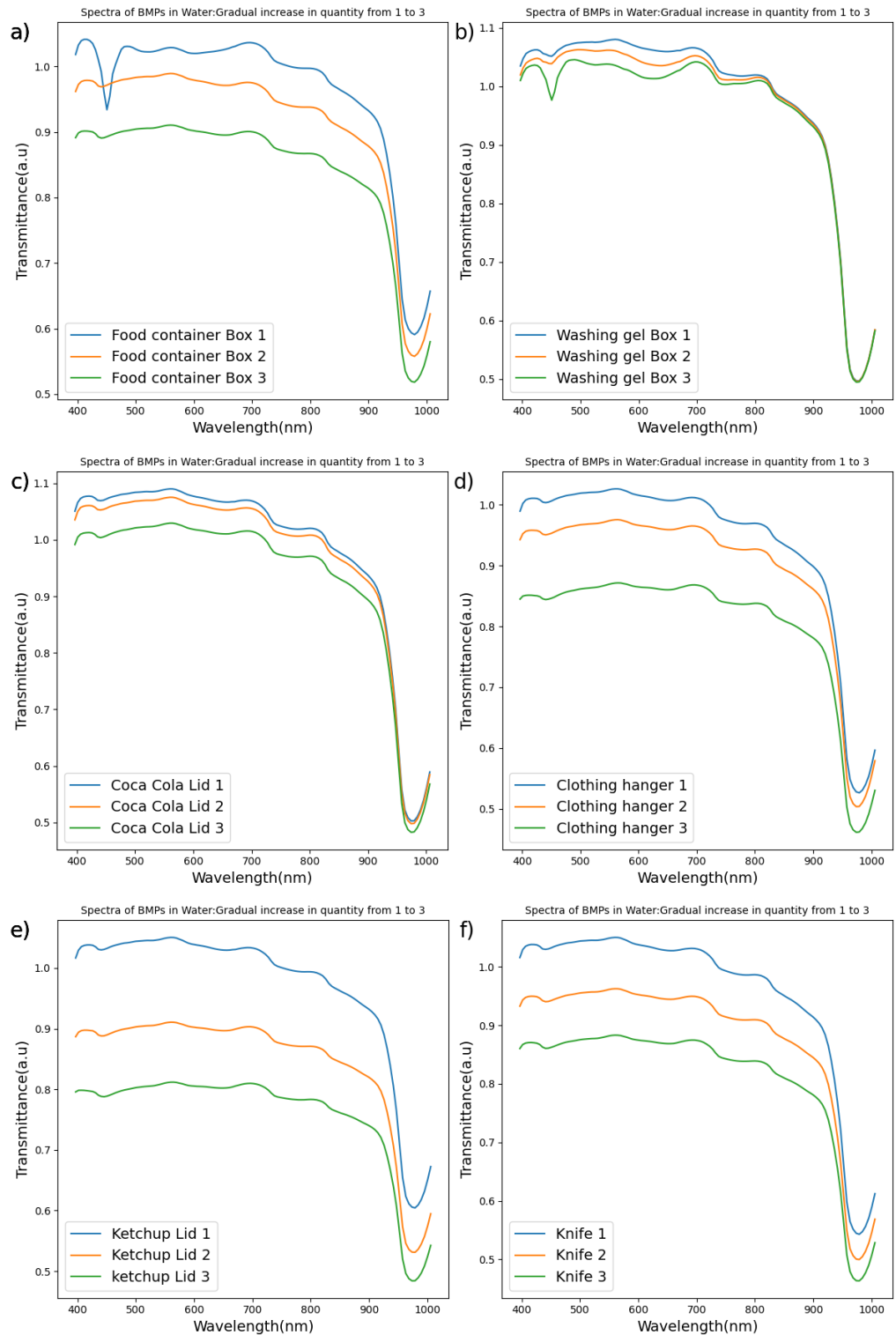
5.2.2.1.1 Quantity-dependent Transmittance of Black Microplastics in Water

In order to comprehensively explore the impact of quantity on the transmittance properties of black microplastics (BMPs) in water using hyperspectral camera, a systematic investigation was conducted in this study. Three different quantities of BMPs were examined to understand their influence on transmittance characteristics. The samples were labeled accordingly in the figure, starting with the minimum quantity represented as 1. Successively, incremental amounts of BMPs were added to the initial quantity, resulting in quantities 2 and 3, respectively, as depicted in Figure 26a).

As larger quantities of BMPs were added, a noticeable decrease in the transmittance peak became evident. This suggests that a greater amount of light was being absorbed by the BMPs as their quantity increased. This behavior was consistently observed across all samples, as depicted in figure 26.

Of particular interest is the sample represented by the blue line in the spectrum. This sample exhibited a higher transmittance spectrum compared to the others, despite having the minimum quantity of BMPs. Conversely, when the maximum quantity of BMPs was added, the transmittance spectrum showed a notable decrease, as depicted by the green spectrum line in the figures. This observation further supports the notion that an increase in BMP quantity leads to a reduction in transmittance, indicating the enhanced light absorption properties of the BMPs.

The findings of this study offer significant insights into the correlation between the quantity of black microplastics (BMPs) and their transmittance properties within water. These results underscore the significance of accounting for the BMP quantity when evaluating their influence on light transmission and absorption in aquatic ecosystems. However, further investigation and analysis are necessary to gain a comprehensive understanding of the underlying mechanisms governing this behavior.



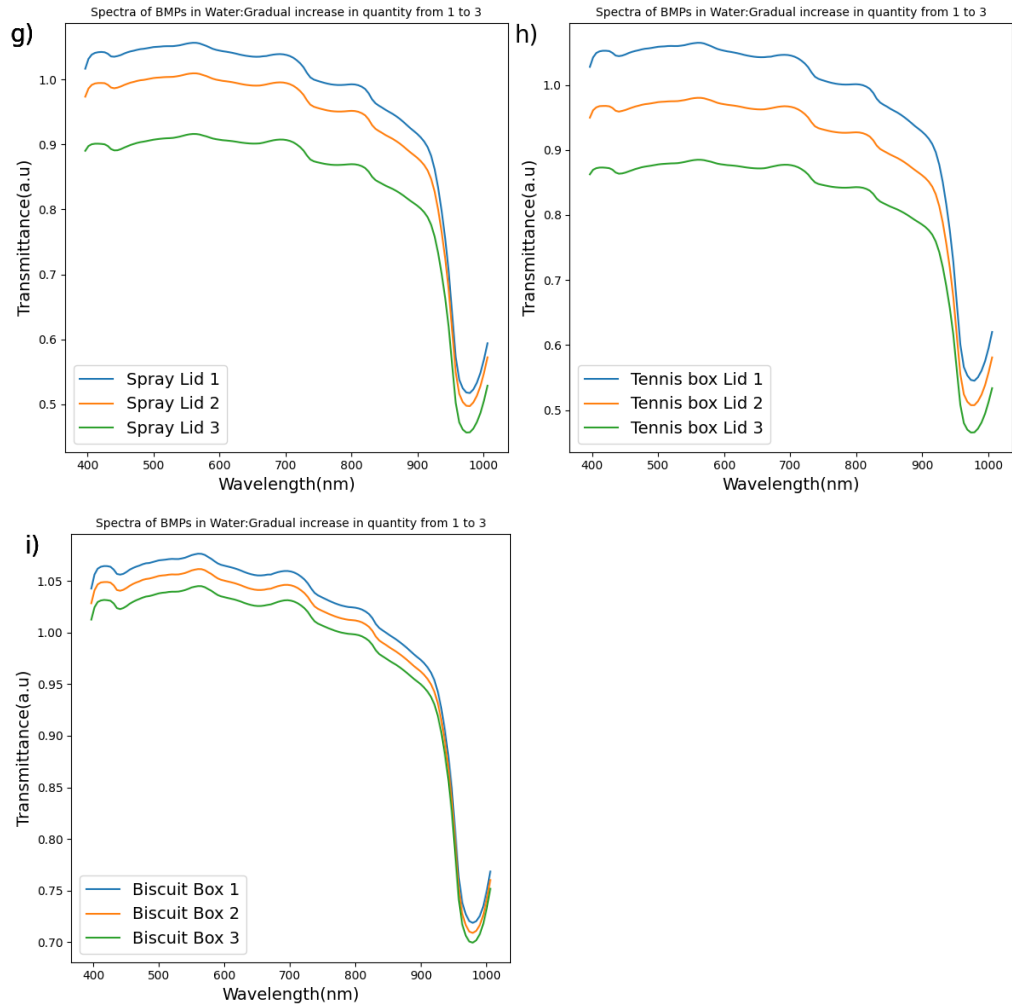


Figure 26: Transmittance in water for BMPs made of piece of a) food container box , b) washing gel box, c) Coca Cola Zero bottle lid, d) clothing hanger, e) ketchup bottle lid, f) Knife, g) spray lid, h) Tennis box lid, and i) Biscuit Box.

5.2.2.2 Reflectance

To investigate the reflectance properties of black microplastics (BMPs) in water, a meticulously chosen set of nine samples was subjected to analysis. The employed spectral camera successfully captured both data and images of the BMPs submerged in water, enabling a comprehensive examination of their reflectance behavior. Python code was employed to process and analyze the collected data, facilitating efficient data analysis and extraction of significant insights.

The initial step involved determining the reflectance characteristics of water in isolation. An average spectrum was computed for a specific region of interest within the water contained in the plate. This region was thoughtfully selected to ensure its representativeness for analysis purposes. The resulting average spectrum, representing the entire green area within the figure 27a, was plotted on the right side figure 27b to facilitate reference and examination.

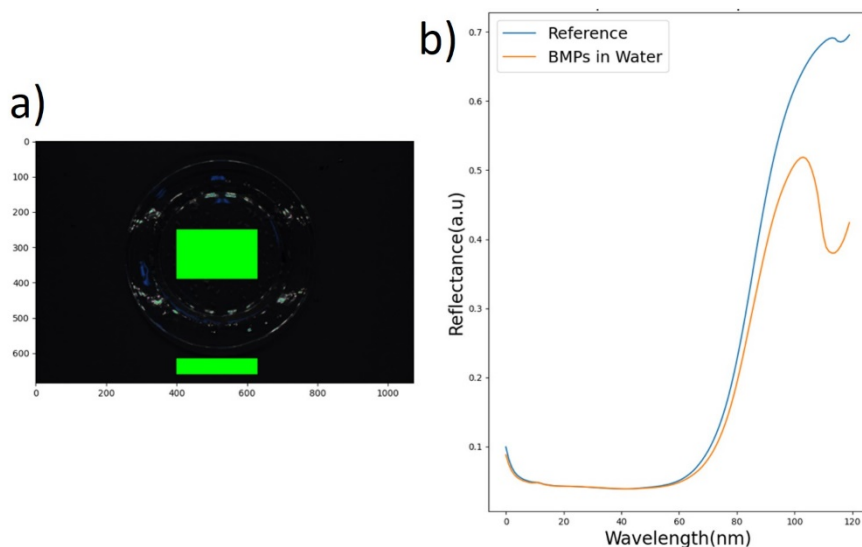


Figure 27: a) Reflectance of BMPs in water and reference green area outside plate. b) Reflectance spectra of water with black microplastics and reference.

To ensure the accuracy and reliability of the findings, the reflectance spectra for both the inside and outside plate regions were plotted and illustrated in figure 27a. Analysis of these spectra revealed that the peak reflectance value inside the plate, when black microplastics were added to the water, was recorded as 0.518. In contrast, the outside plate (labeled as "reference" in the figure) exhibited a slightly higher peak reflectance value of 0.694. Although the discrepancy between these values is relatively small, it remains perceptible. Notably, when black microplastics were absent from the water, the peak reflectance value was measured at 0.538, slightly higher than when BMPs were added.

As a result, we can easily notice a noticeable difference in the reflectance spectra of black microplastics when they are present in the water compared to when they are not. This suggests that the presence of black microplastics in the water has a subtle, but noticeable, effect on how light is reflected.

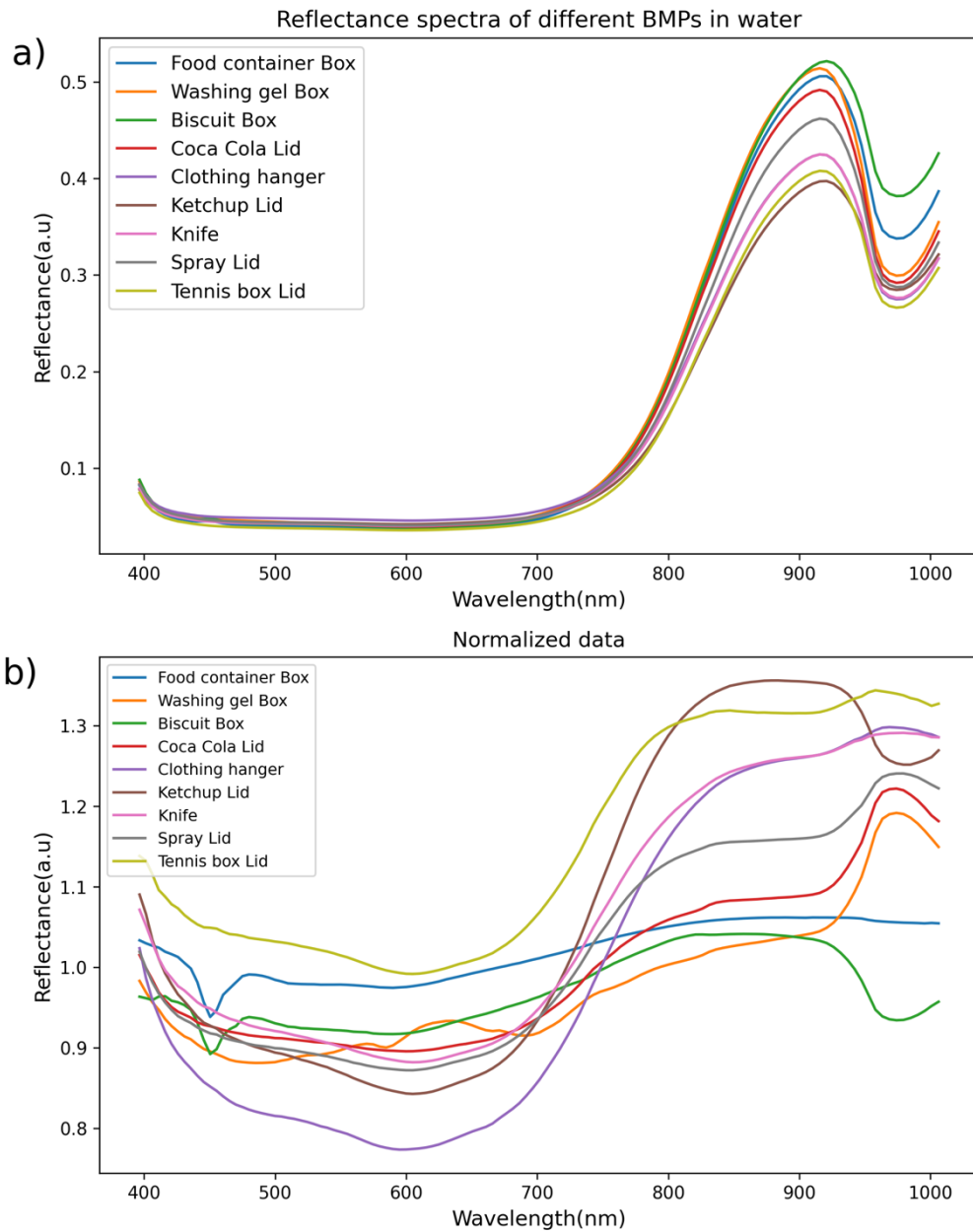


Figure 28: a) Reflectance spectra of different black micro plastics in water b) Normalization of reflectance spectra of different black micro plastics in water

Figure 28a illustrates the reflectance spectra acquired from the analysis of the nine examined samples, while the corresponding normalized data is presented in figure 28b. A notable observation within figure 28a is the subdued nature of the reflectance spectra within the visible range of 400nm to 700nm, which contrasts

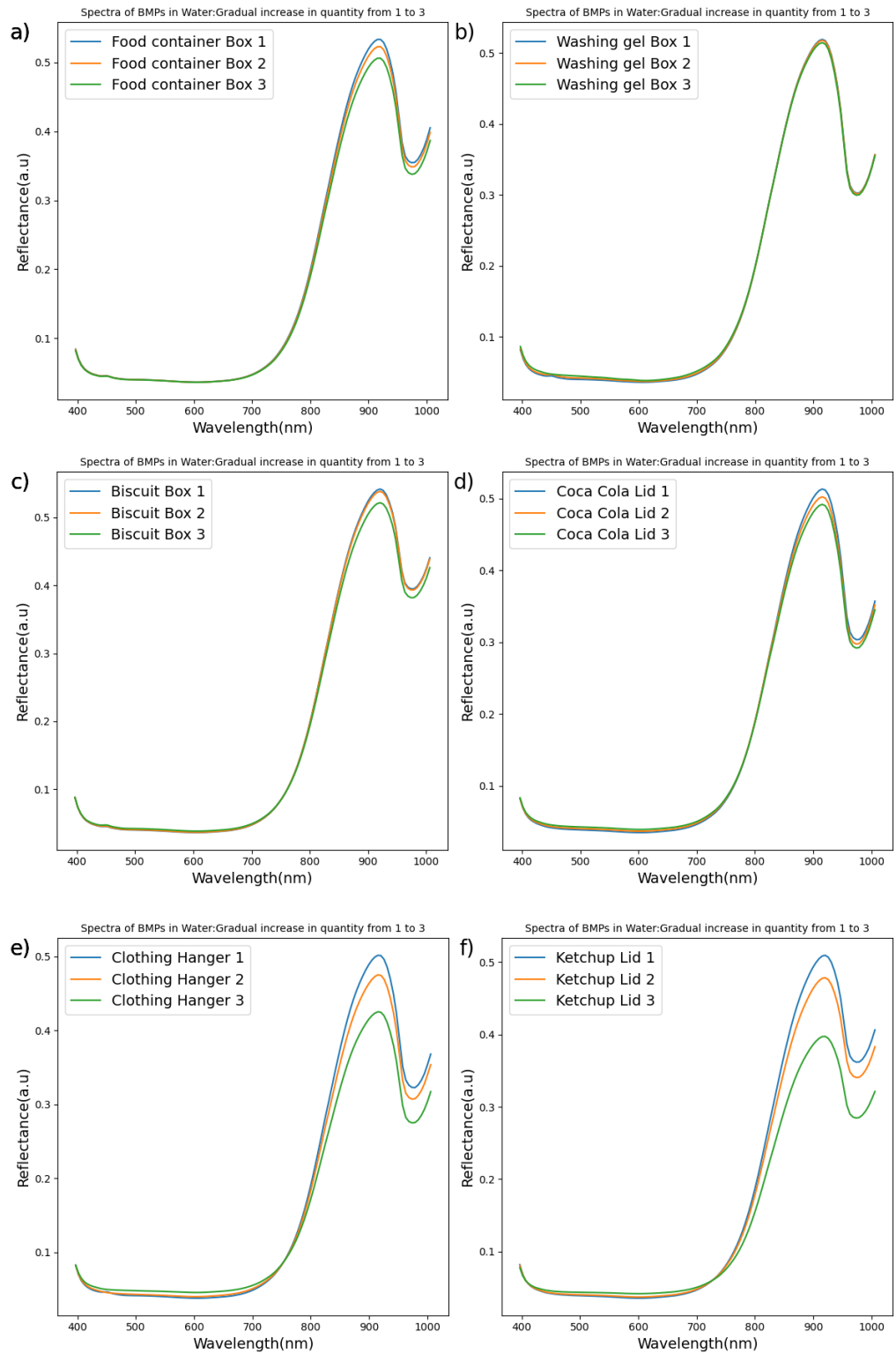
starkly with their substantial augmentation, reaching a peak around the 900nm wavelength.

In figure 28b, each individual sample's distinct spectral signature is evident, signifying the presence of unique optical characteristics within the dataset. Noteworthy among these observations is the elevated reflectance exhibited by the biscuit box sample, setting it apart as the most reflective among all samples. Conversely, the ketchup bottle lid demonstrates the lowest reflectance spectra in comparison to the other examined samples, as depicted in figure 28a. This observation suggests that the reflectance of black microplastics may be influenced by the quantity of BMPs present in the sample, which will be further discussed in the subsequent section on quantity dependence.

5.2.2.2.1 Quantity-dependent Reflectance of Black Microplastics in Water

To comprehensively investigate the influence of quantity on the reflectance properties of black microplastics (BMPs) in water using a hyperspectral camera, a systematic study was conducted. Three different quantities of BMPs were carefully examined to assess their impact on the reflectance characteristics. The corresponding quantities were labeled as 1, 2, and 3 in figures 29, representing the minimum, intermediate, and maximum quantities, respectively.

As the quantity of BMPs increased, a noticeable decrease in the reflectance peak was observed. This suggests that a greater amount of light was being absorbed by the BMPs as their quantity increased. This trend was consistently observed across all samples, as depicted in figure 29.



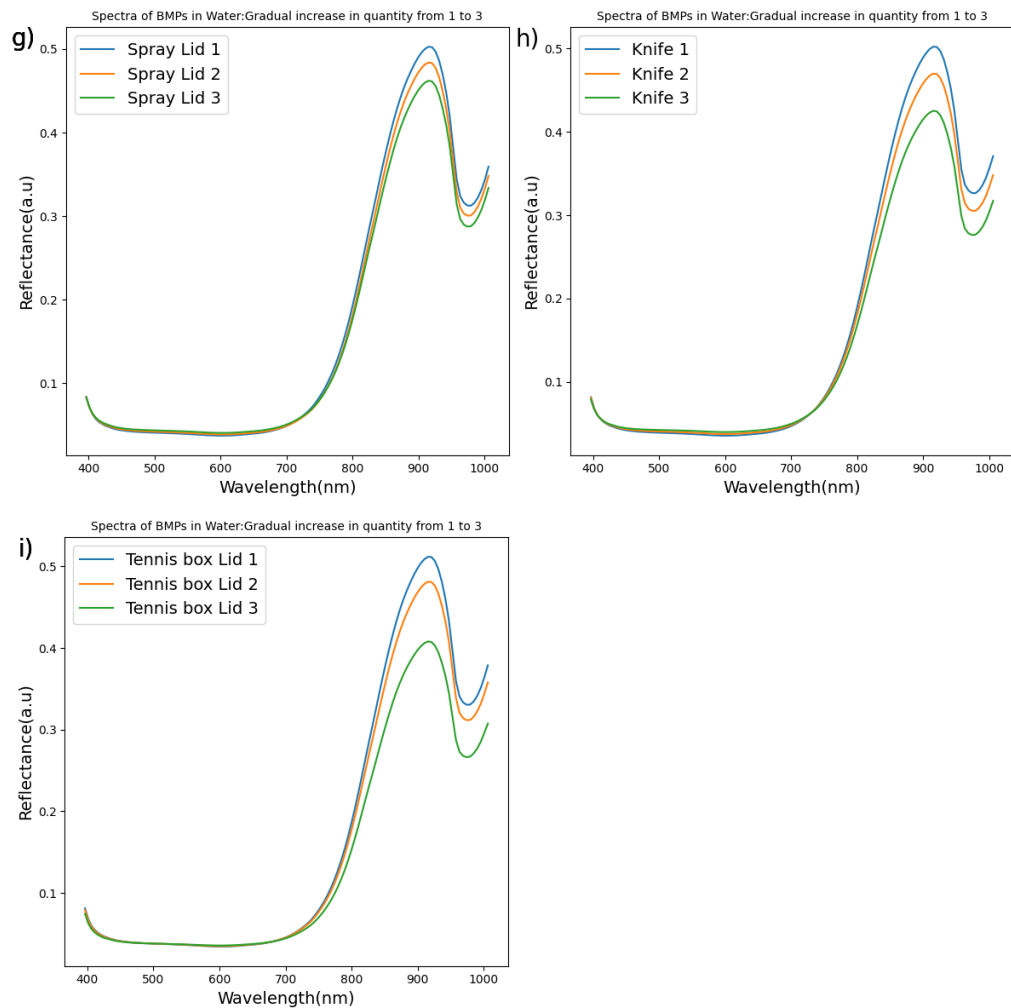


Figure 29: Reflectance of BMPs in water made of pieces of a) Food container, b) Washing gel box, c) Biscuit box, d) Coca Cola Zero bottle lid, e) Clothing hanger, f) ketchup bottle lid, g) Spray lid h) Knife, and i) Tennis box lid.

The results obtained from this study offer valuable insights into how the quantity of black microplastics (BMPs) relates to their reflectance properties in water. These findings emphasize the significance of considering the quantity of BMPs when assessing their influence on light transmission and absorption in aquatic ecosystems. However, further investigation and analysis are required to obtain a comprehensive understanding of the underlying mechanisms that govern these reflectance characteristics. Additionally, such research endeavors are essential to evaluate the implications of these properties for the environmental fate and behavior of black microplastics in water systems.

6 Conclusion

In conclusion, this study has provided valuable insights into the reflectance and transmittance properties of black microplastics in both water and air environments. Through the application of point scanning and hyperspectral imaging techniques, we have illuminated the optical behavior of black microplastics across a range of wavelengths.

In water, the presence of black microplastics was detected in the visible and near-infrared ranges. The study revealed distinct spectral profiles for different black microplastic samples, with unique peak intensities observed in the UV, visible, and near-infrared regions. These findings emphasize the importance of considering variations in sample composition, including different quantities, when evaluating transmittance properties.

Furthermore, our investigation into the reflectance properties of black microplastic in water, using common daily life plastics, included the examination of samples with different quantities. By employing hyperspectral cameras and conducting meticulous analysis, we not only differentiated between samples based on their reflectance spectra but also explored the impact of varying sample quantities. This comprehensive approach enhances our understanding of the reflectance properties of black microplastics and the influence of quantity.

These findings contribute to the broader knowledge of microplastic pollution and its potential consequences for the environment and human health. Future research in this field holds promise for further advancing our comprehension of the behavior and impact of microplastics, ultimately informing mitigation strategies and conservation efforts.

7 Bibliography

- [1] N. Azizi, N. Khoshnamvand, and S. Nasser, "The quantity and quality assessment of microplastics in the freshwater fishes: A systematic review and meta-analysis," *Regional Studies in Marine Science*, vol. 47. Elsevier B.V., Sep. 01, 2021. doi: 10.1016/j.rsma.2021.101955.
- [2] N. Laskar and U. Kumar, "Plastics and microplastics: A threat to environment," *Environmental Technology and Innovation*, vol. 14. Elsevier B.V., May 01, 2019. doi: 10.1016/j.eti.2019.100352.
- [3] S. Nasser and N. Azizi, "Occurrence and Fate of Microplastics in Freshwater Resources," 2022, pp. 187–200. doi: 10.1007/978-3-030-89220-3_9.
- [4] G. Murtaza *et al.*, "A Review Study of Waste-Plastic and Its Deadly Effects on Eco-System," *Imperial Journal of Interdisciplinary Research (IJIR)*, vol. 2, no. 12, 2016.
- [5] Y. Picó and D. Barceló, "Analysis and prevention of microplastics pollution in water: Current perspectives and future directions," *ACS Omega*, vol. 4, no. 4, pp. 6709–6719, Apr. 2019, doi: 10.1021/acsomega.9b00222.
- [6] K. Nogo *et al.*, "Identification of black microplastics using long-wavelength infrared hyperspectral imaging with imaging-type two-dimensional Fourier spectroscopy," *Analytical Methods*, vol. 13, no. 5, pp. 647–659, Feb. 2021, doi: 10.1039/d0ay01738h.
- [7] D. Eerkes-Medrano, R. C. Thompson, and D. C. Aldridge, "Microplastics in freshwater systems: A review of the emerging threats, identification of knowledge gaps and prioritisation of research needs," *Water Research*, vol. 75. Elsevier Ltd, pp. 63–82, May 05, 2015. doi: 10.1016/j.watres.2015.02.012.
- [8] A. D. Vethaak and H. A. Leslie, "Plastic Debris is a Human Health Issue," *Environmental Science and Technology*, vol. 50, no. 13. American Chemical Society, pp. 6825–6826, Jul. 05, 2016. doi: 10.1021/acs.est.6b02569.
- [9] B. Quinn, F. Murphy, and C. Ewins, "Validation of density separation for the rapid recovery of microplastics from sediment," *Analytical Methods*, vol. 9, no. 9, pp. 1491–1498, 2017, doi: 10.1039/C6AY02542K.
- [10] E. M. Crichton, M. Noël, E. A. Gies, and P. S. Ross, "A novel, density-independent and FTIR-compatible approach for the rapid extraction of microplastics from aquatic sediments," *Analytical Methods*, vol. 9, no. 9, pp. 1419–1428, 2017, doi: 10.1039/C6AY02733D.
- [11] R. Lenz, K. Enders, C. A. Stedmon, D. M. A. Mackenzie, and T. G. Nielsen, "A critical assessment of visual identification of marine microplastic using Raman spectroscopy for analysis improvement," *Mar Pollut Bull*, vol. 100, no. 1, pp. 82–91, Nov. 2015, doi: 10.1016/j.marpolbul.2015.09.026.
- [12] J. shan, J. Zhao, L. Liu, Y. Zhang, X. Wang, and F. Wu, "A novel way to rapidly monitor microplastics in soil by hyperspectral imaging technology and chemometrics," *Environmental Pollution*, vol. 238, pp. 121–129, Jul. 2018, doi: 10.1016/j.envpol.2018.03.026.
- [13] W. Becker, K. Sachsenheimer, and M. Klemenz, "Detection of black plastics in the middle infrared spectrum (MIR) using photon Up-conversion technique for polymer recycling purposes," *Polymers (Basel)*, vol. 9, no. 9, Sep. 2017, doi: 10.3390/polym9090435.

- [14] W. W. Hart, P. C. Painter, J. L. Koenig, and M. M. Coleman, "A Fourier Transform Infrared Method of Studying Elastomers Filled with Carbon Black," *Appl Spectrosc*, vol. 31, no. 3, pp. 220–224, May 1977, doi: 10.1366/00037027774463715.
- [15] "FOURIER TRANSFORM INFRARED CHARACTERIZATION OF POLYMERS."
- [16] E. F. Devlin, "The fourier transform infrared spectrum of cured, black-reinforced SBR," *Journal of Polymer Science: Polymer Letters Edition*, vol. 19, no. 4, pp. 189–192, Apr. 1981, doi: 10.1002/pol.1981.130190406.
- [17] J. M. Chalmers, M. W. Mackenzie, J. L. Sharp, and R. N. Ibbett, "Characterization of thin-layer chromatographically separated fractions by Fourier transform infrared diffuse reflectance spectrometry," *Anal Chem*, vol. 59, no. 3, pp. 415–418, Feb. 1987, doi: 10.1021/ac00130a008.
- [18] J. M. Chalmers, M. W. Mackenzie, and N. Poole, "Some observations on FTIR emission spectroscopy of black solid samples," *Mikrochim Acta*, vol. 95, no. 1–6, pp. 249–253, Jan. 1988, doi: 10.1007/BF01349763.
- [19] H. E. Howell and J. R. Davis, "Qualitative Identification of Polymeric Materials Using Near-Infrared Spectroscopy," 1993, pp. 263–285. doi: 10.1021/ba-1993-0236.ch009.
- [20] W. H. A. M. Van Den Broek, D. Wienke, W. J. Melssen, and L. M. C. Buydens, "Optimal Wavelength Range Selection by a Genetic Algorithm for Discrimination Purposes in Spectroscopic Infrared Imaging," *Appl Spectrosc*, vol. 51, no. 8, pp. 1210–1217, Aug. 1997, doi: 10.1366/0003702971941773.
- [21] W. H. A. M. Van Den Broek, D. Wienke, W. J. Melssen, and L. M. C. Buydens, "Plastic material identification with spectroscopic near infrared imaging and artificial neural networks."
- [22] Y. Huang and E. G. Xu, "Black microplastic in plastic pollution: undetected and underestimated?," *Water Emerging Contaminants & Nanoplastics*, vol. 1, no. 3, p. 14, 2022, doi: 10.20517/wecn.2022.10.
- [23] R. Gillibert *et al.*, "Raman tweezers for tire and road wear micro- and nanoparticles analysis," *Environ Sci Nano*, vol. 9, no. 1, pp. 145–161, Jan. 2022, doi: 10.1039/d1en00553g.
- [24] M. Roussey, B. O. Asamoah, and K.-E. Peiponen, "Optical spectroscopy for the detection of micro- and nanoplastics in water," *Photoniques*, no. 110, pp. 40–43, Oct. 2021, doi: 10.1051/photon/202111040.
- [25] J. shan, J. Zhao, L. Liu, Y. Zhang, X. Wang, and F. Wu, "A novel way to rapidly monitor microplastics in soil by hyperspectral imaging technology and chemometrics," *Environmental Pollution*, vol. 238, pp. 121–129, Jul. 2018, doi: 10.1016/j.envpol.2018.03.026.
- [26] A. Turner, "Black plastics: Linear and circular economies, hazardous additives and marine pollution," *Environment International*, vol. 117. Elsevier Ltd, pp. 308–318, Aug. 01, 2018. doi: 10.1016/j.envint.2018.04.036.
- [27] J. Štěpek and H. Daoust, *Additives for Plastics*. New York, NY: Springer New York, 1983. doi: 10.1007/978-1-4419-8481-4.
- [28] A. I. Medalia, "Electrical Conduction in Carbon Black Composites," *Rubber Chemistry and Technology*, vol. 59, no. 3, pp. 432–454, Jul. 1986, doi: 10.5254/1.3538209.

- [29] R. M. Christie, "Pigments, dyes and fluorescent brightening agents for plastics: An overview," *Polym Int*, vol. 34, no. 4, pp. 351–361, Aug. 1994, doi: 10.1002/pi.1994.210340401.
- [30] C. Signoret, A. S. Caro-Bretelle, J. M. Lopez-Cuesta, P. Ienny, and D. Perrin, "MIR spectral characterization of plastic to enable discrimination in an industrial recycling context: II. Specific case of polyolefins," *Waste Management*, vol. 98, pp. 160–172, Oct. 2019, doi: 10.1016/j.wasman.2019.08.010.
- [31] C. Signoret, A. S. Caro-Bretelle, J. M. Lopez-Cuesta, P. Ienny, and D. Perrin, "Alterations of plastics spectra in MIR and the potential impacts on identification towards recycling," *Resour Conserv Recycl*, vol. 161, Oct. 2020, doi: 10.1016/j.resconrec.2020.104980.
- [32] S. Serranti, A. Gargiulo, and G. Bonifazi, "Classification of polyolefins from building and construction waste using NIR hyperspectral imaging system," *Resour Conserv Recycl*, vol. 61, pp. 52–58, Apr. 2012, doi: 10.1016/j.resconrec.2012.01.007.
- [33] M. Balsi, S. Esposito, and M. Moroni, "Hyperspectral characterization of marine plastic litters," in *2018 IEEE International Workshop on Metrology for the Sea; Learning to Measure Sea Health Parameters (MetroSea)*, IEEE, Oct. 2018, pp. 28–32. doi: 10.1109/MetroSea.2018.8657875.
- [34] C. Hibbitts *et al.*, "Dual-band discrimination and imaging of plastic objects," in *Detection and Sensing of Mines, Explosive Objects, and Obscured Targets XXIV*, J. C. Isaacs and S. S. Bishop, Eds., SPIE, May 2019, p. 39. doi: 10.1117/12.2519014.
- [35] M. Moroni, A. Mei, A. Leonardi, E. Lupo, and F. Marca, "PET and PVC Separation with Hyperspectral Imagery," *Sensors*, vol. 15, no. 1, pp. 2205–2227, Jan. 2015, doi: 10.3390/s150102205.
- [36] Z. Chaczko, P. Wajs-Chaczko, D. Tien, and Y. Haidar, "Detection of Microplastics Using Machine Learning," in *2019 International Conference on Machine Learning and Cybernetics (ICMLC)*, IEEE, Jul. 2019, pp. 1–8. doi: 10.1109/ICMLC48188.2019.8949221.
- [37] S. Serranti, "Plastic waste monitoring and recycling by hyperspectral imaging technology," in *SPIE Future Sensing Technologies*, C. R. Valenta and M. Kimata, Eds., SPIE, Nov. 2019, p. 5. doi: 10.1117/12.2549670.
- [38] M. Mehrubeoglu, A. Van Sickle, and J. Turner, "Detection and identification of plastics using SWIR hyperspectral imaging," in *Imaging Spectrometry XXIV: Applications, Sensors, and Processing*, P. Mouroulis and E. J. Lentilucci, Eds., SPIE, Aug. 2020, p. 15. doi: 10.1117/12.2570040.
- [39] A. Faltynkova, G. Johnsen, and M. Wagner, "Hyperspectral imaging as an emerging tool to analyze microplastics: A systematic review and recommendations for future development," *Microplastics and Nanoplastics*, vol. 1, no. 1, Dec. 2021, doi: 10.1186/s43591-021-00014-y.
- [40] P. and G. Geladi, *Multivariate Image Analysis*. John Wiley & Sons, Ltd, 1996.
- [41] P. G. Hans Grahn, *Techniques and Applications of Hyperspectral Image Analysis*. John Wiley & Sons, 2007. Accessed: May 01, 2023. [Online]. Available: <https://books.google.fi/books?hl=en&lr=&id=DqmWQk01mLIC&oi=fnd&pg=PR>

- 5&dq=hyperspectral+imaging+technique&ots=FCjHd6Pjlm&sig=F_jlhT-qQgDdjbXilGP8mQscUsA&redir_esc=y#v=onepage&q&f=false
- [42] J. J. Sahlin and N. A. Peppas, "Near-field FTIR Imaging : A Technique for Enhancing Spatial Resolution in FTIR Microscopy."
 - [43] G. ElMasry and D. W. Sun, "Principles of Hyperspectral Imaging Technology," in *Hyperspectral Imaging for Food Quality Analysis and Control*, Elsevier, 2010, pp. 3–43. doi: 10.1016/B978-0-12-374753-2.10001-2.
 - [44] A. Rogalski, "Optical detectors for focal plane arrays §," 2004.
 - [45] K. I. Schultz *et al.*, "Digital-Pixel Focal Plane Array Technology," 2014.
 - [46] S. Mehta, A. Patel, and J. Mehta, "CCD or CMOS Image sensor for photography," in *2015 International Conference on Communications and Signal Processing (ICCSP)*, IEEE, Apr. 2015, pp. 0291–0294. doi: 10.1109/ICCSP.2015.7322890.
 - [47] S. G. Kazarian and K. L. Andrew Chan, "'Chemical photography' of drug release," *Macromolecules*, vol. 36, no. 26, pp. 9866–9872, Dec. 2003, doi: 10.1021/ma035210l.
 - [48] S. G. Kazarian and K. L. A. Chan, "Sampling approaches in fourier transform infrared imaging applied to polymers," *Prog Colloid Polym Sci*, vol. 132, pp. 1–6, 2006, doi: 10.1007/2882_034.
 - [49] C. Zhu *et al.*, "Characterization of microplastics on filter substrates based on hyperspectral imaging: Laboratory assessments," *Environmental Pollution*, vol. 263, p. 114296, Aug. 2020, doi: 10.1016/j.envpol.2020.114296.

Statement of non-plagiarism

I, Hafiz Ramzan Mubarak, hereby declare that all information in this report has been obtained and presented in accordance with academic rules and ethical conduct and the work I am submitting in this report, except where I have indicated, is my own work.



HAFIZ RAMZAN MUBARAK

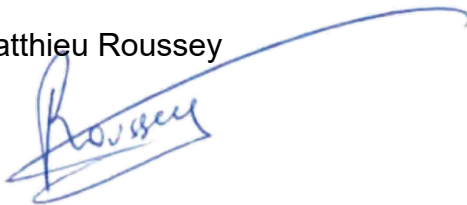
20.08.2023
Joensuu, Finland

Supervisor approval

I, the undersigned, Professor Matthieu Roussey, supervisor of Hafiz Ramzan Mubarak, student of the PSRS EMJMD, during his master thesis at University of Eastern Finland certify that I approve the content of this master thesis report entitled “Hyperspectral imaging of black microplastics in water.”

Date and signature of the supervisor

Matthieu Roussey



Joensuu, 21.08.2023

ELSEVIER LICENSE TERMS AND CONDITIONS

Jul 08, 2023

This Agreement between Hafiz Ramzan Mubarak ("You") and Elsevier ("Elsevier") consists of your license details and the terms and conditions provided by Elsevier and Copyright Clearance Center.

License Number	5584280219792
License date	Jul 08, 2023
Licensed Content Publisher	Elsevier
Licensed Content Publication	Elsevier Books
Licensed Content Title	Hyperspectral Imaging for Food Quality Analysis and Control
Licensed Content Author	Gamal ElMasry, Da-Wen Sun
Licensed Content Date	Jan 1, 2010
Licensed Content Pages	41
Start Page	3
End Page	43
Type of Use	reuse in a thesis/dissertation
Portion	figures/tables/illustrations

Number of figures/tables/illustrations 1

Format electronic

Are you the author of this Elsevier chapter? No

Will you be translating? No

Title student

Institution name university of Eastern Finland

Expected presentation date Aug 2023

Portions figure 1.2

Hafiz Ramzan Mubarak
Peltolankatu 5E 61B

Requestor Location
Joensuu, 80220
Finland
Attn: Hafiz Ramzan Mubarak

Publisher Tax ID GB 494 6272 12

Total 0.00 USD

Terms and Conditions

INTRODUCTION

1. The publisher for this copyrighted material is Elsevier. By clicking "accept" in connection with completing this licensing transaction, you agree that the following terms and conditions apply to this transaction (along with the Billing and Payment terms and conditions established by Copyright Clearance Center, Inc. ("CCC"), at the time that you opened your

RightsLink account and that are available at any time at <https://myaccount.copyright.com>).

GENERAL TERMS

2. Elsevier hereby grants you permission to reproduce the aforementioned material subject to the terms and conditions indicated.

3. Acknowledgement: If any part of the material to be used (for example, figures) has appeared in our publication with credit or acknowledgement to another source, permission must also be sought from that source. If such permission is not obtained then that material may not be included in your publication/copies. Suitable acknowledgement to the source must be made, either as a footnote or in a reference list at the end of your publication, as follows:

"Reprinted from Publication title, Vol /edition number, Author(s), Title of article / title of chapter, Pages No., Copyright (Year), with permission from Elsevier [OR APPLICABLE SOCIETY COPYRIGHT OWNER]." Also Lancet special credit - "Reprinted from The Lancet, Vol. number, Author(s), Title of article, Pages No., Copyright (Year), with permission from Elsevier."

4. Reproduction of this material is confined to the purpose and/or media for which permission is hereby given. The material may not be reproduced or used in any other way, including use in combination with an artificial intelligence tool (including to train an algorithm, test, process, analyse, generate output and/or develop any form of artificial intelligence tool), or to create any derivative work and/or service (including resulting from the use of artificial intelligence tools).

5. Altering/Modifying Material: Not Permitted. However figures and illustrations may be altered/adapted minimally to serve your work. Any other abbreviations, additions, deletions and/or any other alterations shall be made only with prior written authorization of Elsevier Ltd. (Please contact Elsevier's permissions helpdesk [here](#)). No modifications can be made to any Lancet figures/tables and they must be reproduced in full.

6. If the permission fee for the requested use of our material is waived in this instance, please be advised that your future requests for Elsevier materials may attract a fee.

7. Reservation of Rights: Publisher reserves all rights not specifically granted in the combination of (i) the license details provided by you and accepted in the course of this licensing transaction, (ii) these terms and conditions and (iii) CCC's Billing and Payment terms and conditions.

8. License Contingent Upon Payment: While you may exercise the rights licensed immediately upon issuance of the license at the end of the licensing process for the transaction, provided that you have disclosed complete and accurate details of your proposed use, no license is finally effective unless and until full payment is received from you (either by publisher or by CCC) as provided in CCC's Billing and Payment terms and conditions. If full payment is not received on a timely basis, then any license preliminarily granted shall be deemed automatically revoked and shall be void as if never granted. Further, in the event that you breach any of these terms and conditions or any of CCC's Billing and Payment terms and conditions, the license is automatically revoked and shall be void as if never granted. Use of materials as described in a revoked license, as well as any use of the

materials beyond the scope of an unrevoked license, may constitute copyright infringement and publisher reserves the right to take any and all action to protect its copyright in the materials.

9. **Warranties:** Publisher makes no representations or warranties with respect to the licensed material.

10. **Indemnity:** You hereby indemnify and agree to hold harmless publisher and CCC, and their respective officers, directors, employees and agents, from and against any and all claims arising out of your use of the licensed material other than as specifically authorized pursuant to this license.

11. **No Transfer of License:** This license is personal to you and may not be sublicensed, assigned, or transferred by you to any other person without publisher's written permission.

12. **No Amendment Except in Writing:** This license may not be amended except in a writing signed by both parties (or, in the case of publisher, by CCC on publisher's behalf).

13. **Objection to Contrary Terms:** Publisher hereby objects to any terms contained in any purchase order, acknowledgment, check endorsement or other writing prepared by you, which terms are inconsistent with these terms and conditions or CCC's Billing and Payment terms and conditions. These terms and conditions, together with CCC's Billing and Payment terms and conditions (which are incorporated herein), comprise the entire agreement between you and publisher (and CCC) concerning this licensing transaction. In the event of any conflict between your obligations established by these terms and conditions and those established by CCC's Billing and Payment terms and conditions, these terms and conditions shall control.

14. **Revocation:** Elsevier or Copyright Clearance Center may deny the permissions described in this License at their sole discretion, for any reason or no reason, with a full refund payable to you. Notice of such denial will be made using the contact information provided by you. Failure to receive such notice will not alter or invalidate the denial. In no event will Elsevier or Copyright Clearance Center be responsible or liable for any costs, expenses or damage incurred by you as a result of a denial of your permission request, other than a refund of the amount(s) paid by you to Elsevier and/or Copyright Clearance Center for denied permissions.

LIMITED LICENSE

The following terms and conditions apply only to specific license types:

15. **Translation:** This permission is granted for non-exclusive world **English** rights only unless your license was granted for translation rights. If you licensed translation rights you may only translate this content into the languages you requested. A professional translator must perform all translations and reproduce the content word for word preserving the integrity of the article.

16. **Posting licensed content on any Website:** The following terms and conditions apply as follows: Licensing material from an Elsevier journal: All content posted to the web site must maintain the copyright information line on the bottom of each image; A hyper-text must be included to the Homepage of the journal from which you are licensing at <http://www.sciencedirect.com/science/journal/xxxxx> or the Elsevier homepage for books at

<http://www.elsevier.com>; Central Storage: This license does not include permission for a scanned version of the material to be stored in a central repository such as that provided by Heron/XanEdu.

Licensing material from an Elsevier book: A hyper-text link must be included to the Elsevier homepage at <http://www.elsevier.com> . All content posted to the web site must maintain the copyright information line on the bottom of each image.

Posting licensed content on Electronic reserve: In addition to the above the following clauses are applicable: The web site must be password-protected and made available only to bona fide students registered on a relevant course. This permission is granted for 1 year only. You may obtain a new license for future website posting.

17. For journal authors: the following clauses are applicable in addition to the above:

Preprints:

A preprint is an author's own write-up of research results and analysis, it has not been peer-reviewed, nor has it had any other value added to it by a publisher (such as formatting, copyright, technical enhancement etc.).

Authors can share their preprints anywhere at any time. Preprints should not be added to or enhanced in any way in order to appear more like, or to substitute for, the final versions of articles however authors can update their preprints on arXiv or RePEc with their Accepted Author Manuscript (see below).

If accepted for publication, we encourage authors to link from the preprint to their formal publication via its DOI. Millions of researchers have access to the formal publications on ScienceDirect, and so links will help users to find, access, cite and use the best available version. Please note that Cell Press, The Lancet and some society-owned have different preprint policies. Information on these policies is available on the journal homepage.

Accepted Author Manuscripts: An accepted author manuscript is the manuscript of an article that has been accepted for publication and which typically includes author-incorporated changes suggested during submission, peer review and editor-author communications.

Authors can share their accepted author manuscript:

- immediately
 - via their non-commercial person homepage or blog
 - by updating a preprint in arXiv or RePEc with the accepted manuscript
 - via their research institute or institutional repository for internal institutional uses or as part of an invitation-only research collaboration work-group
 - directly by providing copies to their students or to research collaborators for their personal use
 - for private scholarly sharing as part of an invitation-only work group on commercial sites with which Elsevier has an agreement
- After the embargo period
 - via non-commercial hosting platforms such as their institutional repository
 - via commercial sites with which Elsevier has an agreement

In all cases accepted manuscripts should:

- link to the formal publication via its DOI
- bear a CC-BY-NC-ND license - this is easy to do
- if aggregated with other manuscripts, for example in a repository or other site, be shared in alignment with our hosting policy not be added to or enhanced in any way to appear more like, or to substitute for, the published journal article.

Published journal article (JPA): A published journal article (PJA) is the definitive final record of published research that appears or will appear in the journal and embodies all value-adding publishing activities including peer review co-ordination, copy-editing, formatting, (if relevant) pagination and online enrichment.

Policies for sharing publishing journal articles differ for subscription and gold open access articles:

Subscription Articles: If you are an author, please share a link to your article rather than the full-text. Millions of researchers have access to the formal publications on ScienceDirect, and so links will help your users to find, access, cite, and use the best available version.

Theses and dissertations which contain embedded PJAs as part of the formal submission can be posted publicly by the awarding institution with DOI links back to the formal publications on ScienceDirect.

If you are affiliated with a library that subscribes to ScienceDirect you have additional private sharing rights for others' research accessed under that agreement. This includes use for classroom teaching and internal training at the institution (including use in course packs and courseware programs), and inclusion of the article for grant funding purposes.

Gold Open Access Articles: May be shared according to the author-selected end-user license and should contain a [CrossMark logo](#), the end user license, and a DOI link to the formal publication on ScienceDirect.

Please refer to Elsevier's [posting policy](#) for further information.

18. **For book authors** the following clauses are applicable in addition to the above: Authors are permitted to place a brief summary of their work online only. You are not allowed to download and post the published electronic version of your chapter, nor may you scan the printed edition to create an electronic version. **Posting to a repository:** Authors are permitted to post a summary of their chapter only in their institution's repository.

19. **Thesis/Dissertation:** If your license is for use in a thesis/dissertation your thesis may be submitted to your institution in either print or electronic form. Should your thesis be published commercially, please reapply for permission. These requirements include permission for the Library and Archives of Canada to supply single copies, on demand, of the complete thesis and include permission for Proquest/UMI to supply single copies, on demand, of the complete thesis. Should your thesis be published commercially, please reapply for permission. Theses and dissertations which contain embedded PJAs as part of the formal submission can be posted publicly by the awarding institution with DOI links back to the formal publications on ScienceDirect.

Elsevier Open Access Terms and Conditions

You can publish open access with Elsevier in hundreds of open access journals or in nearly 2000 established subscription journals that support open access publishing. Permitted third party re-use of these open access articles is defined by the author's choice of Creative Commons user license. See our [open access license policy](#) for more information.

Terms & Conditions applicable to all Open Access articles published with Elsevier:

Any reuse of the article must not represent the author as endorsing the adaptation of the article nor should the article be modified in such a way as to damage the author's honour or reputation. If any changes have been made, such changes must be clearly indicated.

The author(s) must be appropriately credited and we ask that you include the end user license and a DOI link to the formal publication on ScienceDirect.

If any part of the material to be used (for example, figures) has appeared in our publication with credit or acknowledgement to another source it is the responsibility of the user to ensure their reuse complies with the terms and conditions determined by the rights holder.

Additional Terms & Conditions applicable to each Creative Commons user license:

CC BY: The CC-BY license allows users to copy, to create extracts, abstracts and new works from the Article, to alter and revise the Article and to make commercial use of the Article (including reuse and/or resale of the Article by commercial entities), provided the user gives appropriate credit (with a link to the formal publication through the relevant DOI), provides a link to the license, indicates if changes were made and the licensor is not represented as endorsing the use made of the work. The full details of the license are available at <http://creativecommons.org/licenses/by/4.0>.

CC BY NC SA: The CC BY-NC-SA license allows users to copy, to create extracts, abstracts and new works from the Article, to alter and revise the Article, provided this is not done for commercial purposes, and that the user gives appropriate credit (with a link to the formal publication through the relevant DOI), provides a link to the license, indicates if changes were made and the licensor is not represented as endorsing the use made of the work. Further, any new works must be made available on the same conditions. The full details of the license are available at <http://creativecommons.org/licenses/by-nc-sa/4.0>.

CC BY NC ND: The CC BY-NC-ND license allows users to copy and distribute the Article, provided this is not done for commercial purposes and further does not permit distribution of the Article if it is changed or edited in any way, and provided the user gives appropriate credit (with a link to the formal publication through the relevant DOI), provides a link to the license, and that the licensor is not represented as endorsing the use made of the work. The full details of the license are available at <http://creativecommons.org/licenses/by-nc-nd/4.0>. Any commercial reuse of Open Access articles published with a CC BY NC SA or CC BY NC ND license requires permission from Elsevier and will be subject to a fee.

Commercial reuse includes:

- Associating advertising with the full text of the Article
- Charging fees for document delivery or access
- Article aggregation

- Systematic distribution via e-mail lists or share buttons

Posting or linking by commercial companies for use by customers of those companies.

20. Other Conditions:

v1.10


Questions? customercare@copyright.com.

Home > Microplastics and Nanoplastics > Article

Hyperspectral imaging as an emerging tool to analyze microplastics: A systematic review and recommendations for future development

Review | Open Access | Published: 06 August 2021 | 1 Article number: 13 (2021)

Download PDF 

 You have full access to this open access article



Microplastics and Nanoplastics

[Submit manuscript →](#)

[Andrea Faltynkova](#) , [Geir Johnsen](#) & [Martin Wagner](#)

10k Accesses 25 Citations 62 Altmetric [Metrics](#) [Cite this article](#)

Abstract

A central challenge in microplastics (MP, diameter < 5 mm) research is the analysis of small plastic particles in an efficient manner. This review focuses on the recent application of infrared hyperspectral imaging (HSI) to analyze MP. We provide a narrative context for

Sections

Figures

References

[Abstract](#)

[Introduction](#)

[Methods](#)

[Results & Discussion](#)

[Challenges and Recommendations](#)

[Conclusion](#)